Landslide susceptibility mapping using certainty factor, index of entropy and logistic regression models and their comparison at a landslide prone area in Nepal Himalaya

Krishna Chandra Devkota[1,2], Amar Deep Regmi[3], Hamid Reza Pourghasemi[4], Kohki Yoshida[3], • Biswajeet Pradhan[5], In Chang Ryu[1], Megh Raj Dhital[6], Omar F. Althuwaynee[5]

[1]Department of Geology, Kyungpook National University, 1370 Sankyuk-dong, Buk-gu, Taegu 702-701, Korea

[2]Ministry of Public Administration and Security, National Disaster Management Institute, 136 Mapo-daero, Mapo-gu, Seoul 121-719, Korea

[3]Department of Geology, Faculty of Science, Shinshu University, Asahi 3-1-1, Matsumoto 3908621, Japan

[4]College of Natural Resources & Marine Sciences, Tarbiat Modares University (TMU), Iran

[5]Faculty of Engineering, Spatial and Numerical Modeling Research Group, Department of Civil Engineering, University Putra Malaysia, Serdang, Selangor Darul Ehsan 43400, Malaysia

Tel. +603-89468466; Fax. +603-89468470

[6]Central Department of Geology, Tribhuvan Univeristy, Kritipur, Kathmandu Nepal

Abstract

Landslide susceptibility maps are vital for disaster management and for plan- ning development activities in the mountainous country like Nepal. In the present study, landslide susceptibility assessment of Mugling–Narayanghat road and its surrounding area is made using bivariate (certainty factor and index of entropy) and multivariate (logistic regression) models. At first, a landslide inventory map was prepared using earlier reports and aerial photographs as well as by carrying out field survey. As a result, 321 landslides were mapped and out of which 241 (75 %) were randomly selected for building landslide susceptibility models, while the remaining 80 (25 %) were used for validating the models. The effectiveness of landslide susceptibility assessment using GIS and statistics is based on appropriate selection of the factors which play a dominant role in slope stability. In this case study, the following landslide conditioning factors

were evaluated: slope gradient; slope aspect; altitude; plan curvature; lithology; land use; distance from faults, rivers and roads; topographic wetness index; stream power index; and sediment transport index. These factors were prepared from topographic map, drainage map, road map, and the geological map. Finally, the validation of landslide susceptibility map was carried out using receiver operating characteristic (ROC) curves. The ROC plot estimation results showed that the susceptibility map using index of entropy model with AUC value of 0.9016 has highest prediction accuracy of 90.16 %. Similarly, the susceptibility maps produced using logistic regression model and certainty factor model showed 86.29 and 83.57 % of prediction accuracy, respectively. Furthermore, the ROC plot showed that the success rate of all the three models performed more than 80 % accuracy (i.e. 89.15 % for IOE model, 89.10 % for LR model and 87.21 % for CF model). Hence, it is concluded that all the models employed in this study showed reasonably good accuracy in predicting the landslide susceptibility of Mugling–Narayanghat road section. These landslide suscepti- bility maps can be used for preliminary land use planning and hazard mitigation purpose.

Keywords: Landslide, Susceptibility, Index of entropy, Certainty factor, Logistic regression, GIS, Remote sensing, Nepal

1 Introduction

Nepal lies at the center of 2,400-km-long Himalayan mountain range, which is one of the tectonically most active zones on earth. Among the various land degradation process prevalent in the Himalaya, landslides are one of the most significant phenomena (Ahmad and Joshi 2010) as this region is tectonically very unstable with rugged topography, unstable geological structures, soft and fragile rocks, common earthquakes, along with heavy and prolonged rainfalls during monsoon periods (Deoja et al. 1991; Dhital 2000; DPTC 1996). The study of landslides has drawn worldwide attention mainly due to increasing awareness of its socio-economic impact as well as the increasing pressure of urbanization on the mountain environment (Aleotti and Chowdhury 1999). In Nepal, a significant number of landslides occur each year (as many as 12,000). The impact of artificial structures and human interventions on mountain slopes followed by expansion of agricultural land and watershed management and overgrazing has compounded the land- slide disaster problem in the country (Rajbhandari et al. 2002).

The Mugling–Narayanghat road is one of the vital links of the strategic road network in Nepal. About two-thirds of the highway runs through the right bank of the Trishuli River, and hence, it is vulnerable both to toe cutting by the river and debris deposition by cross drains (Adhikari 2009). This road corridor was severely affected by an extreme rainfall of July 29–30, 2003. The 24-h accumulated rainfall recorded at Bharatpur and Devghat stations was 364 mm and 446 mm, respectively (Adhikari 2009). The incessant and intense rainfall was the causative factor to trigger numerous slides and slope failures along the road section and its surrounding areas. This situation was further worsened during the monsoon of 2006, blocking the traffic for several weeks (DWIDP 2009). To minimize the losses of human life and economic value, potential landslide-prone areas should, therefore, be identified. In this respect, landslide susceptibility assessment can provide valuable information essential for hazard mitigation through proper project planning and implementation.

Landslide susceptibility is the likelihood of a landslide occurrence in an area on the basis of local terrain conditions (Brabb 1984). It is the degree to which a terrain can be affected by slope movements, that is, an estimate of ‘‘where’’ landslides are likely to occur. The advent of remote sensing and GIS has made the landslide susceptibility mapping easier these days (Jia et al. 2010; Karimi Nasab et al. 2010; Bednarik et al. 2012; Wang et al. 2011; Pradhan et al. 2011). Different methods to prepare landslide susceptibility and hazard maps using statistical methods and GIS tools were developed in the last decade (Van Westen et al. 2003; Guzzetti et al. 2005). The most common approaches proposed in the literature are bivariate (Chung and Fabbri 1999; Saha et al. 2005; Pradhan et al. 2006; Magliulo et al. 2008; Pareek et al. 2010; Pradhan and Youssef 2010; Bednarik et al. 2010) and multivariate (Akgűn et al. 2011; Ayalew and Yamagishi 2005; Can et al. 2005; Lee et al. 2007; Gorum et al. 2008; Nefeslioglu et al. 2008; Pradhan 2010a; Pradhan et

al. 2008; Tunusluoglu et al. 2008; Pradhan and Lee 2010c; Oh et al. 2011; Choi et al. 2012), statistical techniques such as the logistic regression (LR). Other different methods have been proposed by several investigators, including weights-of-evidence methods (Bonham-Carter1991; Neuhäuser and Terhorst 2007; Pradhan et al. 2010d; Regmi et al. 2010a; Pourghasemi et al. 2012a, b), modified Bayesian estimation (Chung and Fabbri 1999), weighting factors, weighted linear combinations of instability factors (Ayalew et al. 2004), landside nominal risk factors (Saha et al. 2005), probabilistic-based frequency ratio model (Chung and Fabbri 2003, 2005; Lee and Pradhan 2006, 2007; Akgűn et al. 2008; Pradhan et al. 2010c 2011, 2012), certainty factors (Pourghasemi et al. 2012a), information values (Saha et al. 2005), modified Bayesian estimation (Chung and Fabbri 1999). Among recent models for landslide susceptibility mapping, soft computing techniques such as neuro-fuzzy (Sezer et al. 2011; Vahidnia et al. 2010; Oh and Pradhan 2011), artificial neural networks (Bui et al. 2012a; Lee et al. 2007; Pradhan and Lee 2009, 2010a, b; Pradhan et al. 2010a, b, d; Pradhan and Buchroithner 2010; Pradhan and Pirasteh 2010; Pradhan2011a; Poudyalet al.2010; Yilmaz 2009a, b, 2010a,b; Choiet al.2012; Zarea et al. 2012), fuzzy-logic (Akgu ¨n et al. 2012; Bui et al. 2012b; Ercanoglu and Gokceoglu 2002; Kanungo et al. 2008; Pradhan 2010b, 2010c, 2011b; Pradhan et al. 2009; Pourghasemi et al. 2012c) can be seen in the literature. Additionally, there exists some other data mining techniques such as support vector machine (SVM) (Bui et al. 2012c; Brenning 2005; Yilmaz 2010a), decision tree methods (Saito et al. 2009; Nefeslioglu et al. 2010), spatial decision support system (SDSS) (Wan 2009), spatial multi-criteria evaluation (SMCE) (Pourghasemi et al. 2012d), index of entropy (Bednarik et al. 2010; Constantin et al. 2011; Pourghasemi et al. 2012e), evidential belief function (EBF) (Althuwaynee et al. 2012), etc. to evaluate the landslide susceptibility, to overcome shortcomings in the above-mentioned methods.

The aim of this paper is to produce landslide susceptibility map of Mugling–Narayanghat road corridor using two bivariate statistical models [certainty factor (CF), index of entropy (IOE)] and one multivariate statistical model [logistic regression (LR)]. These models exploit information obtained from the inventory map to predict where landslides may occur in future. These models are tested, and the results are discussed. In literature, various bivariate and multivariate approaches for landslide susceptibility exist. However, a comparison of these approaches is not commonly encountered. This contribution provides originality to this study.

2 The study area

The 36-km-long Mugling–Narayanghat road is located in a mountainous terrain of Central Nepal, in the Chitwan District of the Narayani Zone. The study area (longitude 84°26′00″ E to 84°34′30″ E and latitude 27°51′30″ N to 27°45′30″ N) falls within the topographical map 2784-03C (Mugling) and 2784-02D (Jugedi Bajar) and covers an area of about 65 km^2 (Fig. 1). The minimum and maximum altitudes of the area vary from 200 m at Jugedi Bajar and 1,380 m in the vicinity of Mulethumki and Chaur.

Brunsden et al. (1975) were one of the first to develop a geomorphological map of a road corridor in Nepal. Kojan (1978) studied the landslide problems along the Godavari–Dandeldhura road. He identified the main hazardous areas along the road section and recommended various methods of slope stabilization. Wagner (1981) was the first to prepare a landslide and gully erosion hazard map based on field observation in Nepal. Many researchers tried to establish linkage between landslides and human activities (Gerrard 1994). In Himalayas, this link forms a major component of what is known as Himalayan Environmental Degradation Theory (Ives and Messerli 1981). From the airborne survey of Nepal, Laban (1979) concluded that geological structure and lithology accounted for more than 70 % of landslides occurrences in this region.

Deoja et al. (1991) further developed this method and proposed various ratings for attributes such as rock type, soil type, slope angle, relative relief, groundwater, surface hydrology, folds, and faults. The first detailed landslide hazard mapping was carried out along the Tulsipur–Sallyan, Ghorahi–Piuthan, and Piuthan– Libang roads of mid-west Nepal (DoR/USAID 1986). These maps were derived from engineering geological maps of the road alignment on a scale of 1:5,000, aerial photo interpretation, and kinematic analysis of joints. Feasibility- and detailed-stage landslide hazard mappings were carried out along the Baitadi–Darchula road alignment in far west Nepal (Dhital et al. 1991). According to Shroder and Bishop (1998), landslides in the Himalaya are scale-dependent and range from massive extent of a whole mountain range (gravity tectonics) through the failure of single peaks to very minor slope failures. Gerrard and Gardner (2000a, b) suggested that there is a clear anthropogenic influence in the occurrence of landslides in the mountainous areas of Nepal. Recently, many researchers have applied various GIS-based statistical techniques in the landslide susceptibility mapping in various parts of Nepal Himalaya (Dhital et al. 2006; Dahal et al. 2008, 2012; Poudyal et al. 2010; Regmi et al. 2010b; Dhakal et al. 2000). Some work has been done on the role of rock weathering and clay minerals in landslide formation in Nepal Himalaya (Regmi et al. 2012 and Hasegawa et al. 2009). Rainfall threshold for landslides in certain part of Nepal was calculated by Dahal and Hasegawa (2008). Petley et al. (2006) analyzed a database of landslide fatalities in Nepal from 1978 to 2005 and found that there is a high level of variability in the occurrence of landslides from year to year, but its overall trend is increasing.

3 Geological and Morphological Setting

The Mugling–Narayanghat road passes through the Precambrian Lesser Himalayan rocks of the Nawakot Complex (Stőcklin and Bhattarai 1978; Stőcklin 1980), the Miocene Siwaliks and

Holocene alluvial deposits (Fig. 2). The Nawakot Complex is divided into the Lower Nawakot Group and Upper Nawakot Group, and along this road section, the rocks from both the groups are observed. The main rock types are mudstones, sandstones, limestones, dolomites, slates, phyllites, quartzites, and amphibolites. A majority of instabilities were observed within the Nourpul Formation. The Kuncha Formation, Fagfog Quartzite, Dandagaun Phyllite, Nourpul Formation, and Dhading Dolomite are from the Lower Nawakot Group, while Benighat Slates represents the Upper Nawakot Group. The Purebesi Quartzite Member is a distinct quartzite zone, overlying the phyllites of the Dandagaun Formation, and forms the basal part of the Nourpul Formation. Apart from this, some amphibolite bands are also observed within the Nourpul Formation. The Siwalik Group in the study area consists of the Lower Siwaliks and Middle Siwaliks (Ganser 1964). The Holocene deposits consist of river terraces of different ages. The main rock types are mudstones, sandstones, limestones, dolomites, slates, phyllites, quartzites, and amphibolites. Majority of instabilities were observed within Nourpul Formation rocks. The main geological structures that demarcate the study area are the Main Boundary Thrust (MBT), Jugadi Thrust (JT), Kamalpur Thrust (KT), Simaltal Thrust (ST), and Virkuna Thrust (VT). All the thrusts are trending in east–west direction. The MBT is a major fault separating the Lesser Himalaya to the north from the Siwaliks to the South (Fig. 2).

The highway between km 23 and km 28 lies within this thrust zone, where thick colluviums and plenty of seepage are observed. Geomorphologically, Nepal is divided into the following eight units running east–west: the Terai, Churia Range, Dun Valley, Mahabharat Range, Midland, Fore Himalaya, Higher Himalaya, Inner and Trans Himalaya (Hagen 1969) and the Mugling–Narayanghat road lies within the Mahabharat Range, Churia Range, and Dun Valley. The southernmost tableland belongs to the Dun Valley and is covered by various alluvial deposits.

Here, the slope is gentle and the elevation is subdued. As the alluvium covers most of the Siwaliks composing the Churia Range, they are exposed only on the riverbanks, where the stream erosion is intense. Most of the study area belongs to the Mahabharat Range, which lies to the north of the Churia Range and consists of higher mountains with steeper slopes.

4 Landslide inventory map

Understanding the role of individual factors controlling landslide location, geographical pattern, and spatial density is important to predict where landslides can occur in the future, that is, to ascertain landslide susceptibility (Varnes 1984; Soeters and Van Westen 1996; Guzzetti et al. 1999, 2005). A landslide inventory map is one that identifies the definite location of the existing landslides along with its type and the time of occurrence (Wieczorek 1984; Einstein 1988; Soeters and van Westen 1996). The first step in landslide susceptibility assessments is to acquire information about the landslides that have occurred in the past. This stage is considered as the fundamental part of the landslide hazard studies (Guzzetti et al. 1999; Ercanoglu and Gokceoglu 2004). Since landslide occurrences in the past and present are keys to spatial prediction in future (Guzzetti et al. 1999), a landslide inventory map is a prerequisite for such a study. A landslide inventory map provides the basic information for evaluating landslide hazards or risk. Accurate detection of the location of landslides is very important for probabilistic landslide susceptibility analysis. The landslides on the Mugling–Narayanghat road were identified from the interpretation of aerial photographs (taken after the monsoon of 2003), satellite images and were verified in the field. In total, 321 landslides were mapped (Fig. 1) and subsequently digitized for further analysis. The mapped landslides cover an area of 2.05 km2, which constitutes 3.15 % of the entire study area, where the dominant failure is of rotational type (Fig. 3). Rock falls, debris flow, and topples are also observed along the highway (Fig. 3). From these landslides, 241

(75 %) randomly selected instabilities were taken for making land- slide susceptibility models and 80 (25 %) were used for validating the models.

5 Landslide conditioning factors

The factors controlling instabilities considered in the present study are slope gradient, slope aspect, plan curvature, altitude, stream power index (SPI), topographic wetness index (TWI), stream sediment transport index (STI), geology, land use, distance from faults, distance from rivers, and distance from roads. A short description of each thematic map is given below. The geomorphic factors like slope gradient, slope aspect, plan curvature, altitude, SPI, TWI, and SPI were obtained from the DEM produced by the topographic map of 1:25,000 scale provided by the Department of Survey, Nepal. The land use map was also provided by the Department of Survey, Nepal. Geological map was prepared in the field based on the geological map of Central Nepal (Stőcklin and Bhattarai 1978; Stőcklin 1980). The geological maps were also useful for the delineation of major faults in the study area. The distance from rivers and the distance from roads maps were produced, respectively, from the drainage map and the topographic map using ArcGIS 9.3. Brief description of each thematic map used in the present study is given below.

5.1. Slope gradient

The slope gradient is one of the most important factors that influence slope stability (Bednarik et al. 2009). In general, stability of slope is the interplay of slope angle with material properties such as friction angle, permeability, and cohesion. Slope gradient map was derived from DEM of 20 9 20 (m) grid size. The original slope angle values vary between 0° and 79.54°, and the values were reclassified into 5 categories (Fig. 4a) which are most widely used subdivisions in Nepal and other southeast Asian countries (Pradhan and Lee 2010a; Dhital et al. 2006; Saha et al. 2005).

5.2 Slope aspect

The slope aspect or the direction of maximum slope of the terrain surface is divided into nine classes (Fig. 4b). Although the relation between the aspect and the mass movement has been investigated for a long time, no general decision could have been given regarding the aspect–landslide relationship (Ercanoglu et al. 2004). However, it is emphasized that the aspect is one of the significant factors producing the landslide susceptibility maps (Lee et al. 2004. Physically, the aspect is related to the parameters such as the orientation of discontinuities controlling landslides, precipitation, wind impact, and exposition to sun- light (Ercanoglu et al. 2004).

5.3 Plan curvature

The curvature values represent the morphology of the topography (Lee and Min 2001; Lee et al. 2004; Erener and Dűzgűn 2010). The curvature maps (Fig. 4c) were obtained from the second derivative of the surface.

5.4 Altitude

Altitude is another frequently used parameter for landslide susceptibility studies. It is stated that the landslides have more tendency to occur at higher elevations (Ercanoglu et al. 2004). In the study area, the elevation ranges between 200 and 1,380 m. The elevation values were divided into eight categories with an interval of 150 m. (Fig. 4d).

5.5 Stream power index (SPI)

SPI measures the erosion power of the stream and is also considered as a factor contributing toward stability within the study area. The SPI can be defined as (Moore and Grayson 1991):

$$SPI = A_s \tan \beta \qquad (1)$$

where As is the specific catchment area and β is the local slope gradient measured in degrees. In the present study, SPI is divided into 4 classes (Fig. 4e).

5.6 Topographic wetness index (TWI)

The topographic wetness index (TWI), which combines local upslope contributing area and the entire slope, is commonly used to quantify topographic control on hydrological processes. It is expressed as:

$$TWI = \ln\left(\frac{a}{\tan\beta}\right) \qquad (2)$$

where a is the cumulative upslope area draining through a point (per unit contour length) and tanβ is the slope angle at the point. It affects the spatial distribution of soil moisture, and the groundwater flow often follows surface topography. In this study, TWI was considered as another contributing factor (Fig. 4f).

5.7 Sediment transport index (STI)

The sediment transport index (STI) characterizes the process of erosion and deposition. In the present study, STI is divided into 4 classes (Fig. 4g).

5.8 Land use map

Land use also plays a significant role in the stability of slope. The land covered by forest regulates continuous water flow and water infiltrates regularly, whereas the cultivated land affects the slope stability due to saturation of covered soil. Based on field observations and mapping, the following nine classes are considered: cutting, cultivation, forest, orchard, grass, bush, sand barren, and river (Fig. 4k). Bush (37 %) covers the highest amount of area followed by cutting (31 %) and cultivation lands (29 %).

5.9 Lithology

Lithology plays an important role in landslide susceptibility studies because different geological units have different susceptibilities to active geomorphic processes of the Himalaya (Pradhan et al. 2006). The sediments and rocks in this watershed belong to Holocence alluvial deposits, Miocene Siwaliks, and Precambrian Lesser Himalaya and consist of sandstone, siltstone, mudstone, conglomerate, limestone, dolomite, slate, phyllite, quartzite, and amphibolites (Fig. 2).

5.10 Distance from faults

Faults are the tectonic breaks that usually decrease the rock strength. These dislocations are responsible for triggering a large number of landslides on the Mugling–Narayanghat road. Fault lines were derived from the geological map of the region. In the present study, the distance from fault map was reclassified into 6 divisions (Fig. 4j).

5.11 Distance from rivers

Runoff plays an important role as a triggering factor for landslides. On the basis of rivers and streams, a map of proximity to drainage was generated using Arc GIS 9.3. In the present study, the distance from river map is divided into 5 categories (4 h).

5.12 Distance from roads

The roads built on the slopes cause the loss of toe support. The change of the topography and the loss of support lead to the increase of strain behind the slope and the development of cracks. Instabilities occur in the slope because of the negative effects such as water infiltration afterward. Also, a given road segment may act as a barrier, a net source, a net sink or a corridor for water flow, and depending on its location in the area, it usually serves as a source of landslides (Pradhan et al. 2010a). The detail road network map provided by the Department of Survey, Nepal, was used to generate the distance from roads map (Fig. 4i).

6 Modeling approach

6.1 Certainty factor model

Certainty Factor (CF) is a model that has been applied by different researchers in landslide susceptibility mapping (Kanungo et al. 2011; Go ¨kc¸eoluetal. 2005). The CF approach is one of the possible proposed favorability functions to handle the problem of combining different data layers and the heterogeneity and uncertainty of the input data. The certainty factors (CF) are given by the following equation:

$$CF_{ij} = \begin{cases} \dfrac{f_{ij} - f}{f_{ij}\,(1 - f)} & if\ f_{ij} \geq f \\ \dfrac{f_{ij} - f}{f(1 - f_{ij})} & if\ f_{ij} \leq f \end{cases} \qquad (3)$$

where CFij is the certainty factor given to a certain class i of parameter j. fij is the conditional probability having a number of landslide event occurring in class i of parameter j and f is the prior probability having total number of landslide event occurring in the study area.

The value of the certainty factor ranges between -1 and +1. The minimum -1 means definitely false and +1 means definitely true. A positive value means an increasing certainty in landslide occurrence, while a negative value corresponds to a decreasing certainty in landslide occurrence. A value close to 0 means that the prior probability is very similar to the conditional one; hence, it is difficult to give any indication about the certainty of the landslide occurrence (Pourghasemi et al. 2012e).

The CF values for all the condition factors were calculated by overlying landslides with the parameter class, that is, by calculating the landslide density and the CF values of all the layers using Eq. 3. Next, the CF values of the landslide conditioning factors were used for creating various CF layers (Table 1). Then, the calculated CF layers were combined pairwise. The

combination of two CF values, X and Y, due to two different layers of information, is expressed as Z in Eq. 4, given below:

$$Z = \begin{cases} X + Y - XY & X, Y \geq 0 \\ \frac{X+Y}{1-\min(|X|,|Y|)} & X, Y\ O\ pposite\ sign \\ X + Y + XY & X, Y < 0 \end{cases} \quad (4)$$

The pairwise combination is performed repeatedly until all the CF layers are added to obtain the landslide susceptibility index (LSI). To make the results easier to interpret, the LSI values are grouped into susceptibility classes to create landslide susceptibility zonation map for the study area. Several authors have applied various methods for dividing the LSI map. In this study, natural break classification method (Constantin et al. 2011; Xu et al. 2012) was used to divide the interval into four classes and a susceptibility map was prepared. Subsequently, the same classification approach was used for index of entropy and logistic regression models.

6.2 Index of entropy model

The second model used for evaluating the landslide susceptibility in the present study is the bivariate index of entropy model (Van Westen 2004). The method is based on the principle of bivariate analysis, where the density of landslides within a certain parameter is deter- mined. This approach allows calculation of the weight for each input variable. In the present model, the weighting process is based on the methodology proposed by Vlcko et al. (1980). The weight value for each parameter taken separately is expressed as an entropy index.

The weight parameter was obtained from the defined level of entropy representing the approximation to normal distribution of the probability. The entropy index indicates the extent of disorder in the environment. It also expresses which parameters in a natural environment are most relevant for the development of mass movements (Bednarik et al. 2010). The equations

used to calculate the information coefficient Wj representing the weight value for the parameter as a whole are:

$$P_{ij} = \frac{A_{sd}}{A_t} \qquad (5)$$

$$\left(P_{ij}\right) = \frac{P_{ij}}{\sum_{j=1}^{s_j} P_{ij}} \qquad (6)$$

Here, H_j and $H_{j\,max}$ are the entropy values (Eqs. 7 and 8) and they are written as;

$$H_j = -\sum_{i=1}^{s_j} (P_{ij}) \log_2\left(P_{ij}\right), \quad j = 1, \ldots\ldots, n \qquad (7)$$

$$H_{j\,max} = \log_2 s_j, \qquad s_j\ is\ the\ munber\ of\ classes \qquad (8)$$

I_j is the information coefficient (Eq. 9) and W_j represents the resultant weight value for the parameter as a whole (Eq. 10).

$$I_j = \frac{H_{jmax} - H_j}{H_{jmax}} \qquad (9)$$

$$W_j = I_j \times P_j \qquad (10)$$

The result varies from 0 – 1. The closer the value is to the number 1, the greater the instability is.

Here, P_j is the slope failure probability for (j=1... n). The complete calculation of weight determination for individual parameters is presented in Table 2. The final susceptibility value is expressed by the sum of all parameter classes, ranked according to the calculated landslide density for each class. It is expressed as;

$$y = \sum_{i=1}^{n} \frac{z}{m_i} \times C \times W_j \qquad (11)$$

where y is the sum of all the classes; i is the number of particular parametric map (1,2, ...n); z is the number of classes within parametric map with the greatest number of classes; m_i is the number of classes within particular parametric map; C is the value of the class after secondary classification and W_j is the weight of a parameter.

6.3 Logistic regression model

Logistic regression allows forming a multivariate regression relation between a dependent variable and several independent variables. The dependent variable is dichotomous, while the independent variable can be interval, dichotomous, or categorical (Atkinson and Massari 1998). In the present situation, the dependent variable is a binary variable representing the presence or absence of landslides. The logistic model can be expressed in its simplest form as:

$$p = \frac{\exp(z)}{(1 + \exp(z)} \qquad (12)$$

where p is the probability of an event (landslide) occurrence, which varies from 0 to 1 on an s-shaped curve; z is defined as the following equation (linear logistic model), and its value varies from $-\infty$ to $+\infty$:

$$Z = \beta_0 + \beta_1 X_1 + \beta_2 X_2 + \ldots + \beta_n X_n \qquad (13)$$

where 0 represents the intercept of model, 1;2;... ;n the partial regression coefficients, X1; X2; ...; Xn represent the independent variables. The logistic regression model involves fitting of Eq. 13 to the data and then expressing the probability of the presence/absence of landslides in each mapping unit. The relative contribution of each mapping unit to the logistic function can be obtained by looking at the significance of each regression parameter. The logistic regression analysis was performed using the SPSS statistical software. Firstly, all the conditioning factors

and landslides were converted into grid format, and then, these grid maps are converted into ACSII data format (Acronym for the American Standard Code for Information Interchange). The ASCII data of each map was exported to SPSS, and then the logistic regression model was run to obtain the coefficients of the landslide conditioning factors.

7 Results and discussion

7.1 Certainty factor (CF) model

The correlation between the location of landslides and the landslide conditioning factors was performed. The final landslide susceptibility map obtained by CF model is shown in Fig. 5. The CF values were reckoned for all conditioning factors by overlaying and calculating the landslide frequency (Table 1). Then, the CF values of twelve landslide conditioning factors were determined using Eq. 3. The results of spatial relationship between landslide and conditioning factors using CF model are given in Table 1.

The slope class 35°–45° has the highest value of CF (0.31) followed by 25°–35° class (0.26). The lowest value of CF (-0.82) is for slope class 0°–15°. From this, it is clear that the landslide occurrence increases by the increase in slope gradient up to a certain extent, and then, it decreases. Few landslides occur on a very gentle slope and the landslide occurrence decreases as the slope becomes higher than 45————————————. In the case of slope aspect, the CF value is positive for east to southwest-facing slope facing, with the maximum value (0.42) at southeast-facing slope followed by south-facing (0.37) slope. The north-facing slopes are less prone to landslides as they have negative CF value. The CF values of altitude show that they are positive for the ranges of <350, 350–500, 500–650, 650–800, with the highest value (0.29) for the altitude ranging between 350 and 500 m. The CF value decreases with both the increase and decrease in altitude. It becomes negative after 800 m. This shows that the probability of landslide

occurrence decreases as the altitude becomes higher than 800 m. In the case of curvature, the CF value is positive (0.03) only on concave slopes. The convex and flat slopes are not responsible for landslide hazard in this area. For the geology, it can be seen that the Middle Siwaliks (CF = 0.9), Lower Siwaliks (CF = 0.63), Purebesi Quartzite (CF = 0.28), alluvial deposits (CF = 0.26), and amphibolites (CF = 0.07) are found to be more susceptible to sliding (Table 1). In the case of land use, positive value of CF is seen only on cultivation land. This may be due to the unplanned excavation of slope during agricultural activities, as well as due to the increase in moisture content during the irrigation process. In the case of distance from faults, the intervals 100–200, 200–300, 300–400, and 400–500 m have weights (CF) of 0.2, 0.08, 0.11 and 0.654, respectively. The influence of drainage system upon the landslide susceptibility was also analyzed by identifying the drainage river line by buffering. The distance range of 0–50 m (0.17) has the highest CF value, followed by 0–100 m (0.002). This indicates that the landslide occurrence decreases with the increase in distance from the river. In the case of distance form roads, the intervals 150–200 (0.23) and 200–250 (0.33) have higher CF values, that is, the landslide susceptibility is higher in these ranges. The relation between TWI landslide probabilities showed that 0–8 class has the highest value of CF (0.12), and for SPI, the class of 150–300 shows a high CF value (0.24). Similarly, for sediment transport index, the highest CF value was obtained for the interval of 40–120 m.

7.2 Index of Entropy (IOE) Model

The procedure for calculating the final weight Wj of the conditioning factors is explained in the earlier section, and the result is presented in Table 2. The final landslide susceptibility map was prepared by summing of weighted multiplications of the secondarily reclassified conditioning factors maps as given by Eq. 14 (Fig. 6)

$$y = slope_{reclass} * 0.101 + aspect_{reclass} * 0.287 + altitude_{reclass} * 0.344 + geolog_{reclass} * 0.536 + fault_{reclass} * 0.008 + river_{reclass} * 0.014 + road_{reclass} * 0.021 + TWI_{reclass} * 0.025 + SPI_{reclass} * 0.052 + STI_{reclass} * 0.039 + land\ use_{reclass} * 0.174 \quad (14)$$

From the result (Pij), it is seen that slope interval of 35°–45° is highly prone to landslide followed by the slope class 25°–35°. In the case of aspect, southeast-facing slopes followed by south-facing, east-facing, and southwest-facing slopes are susceptible to landsliding. From the Wj value, it is seen that the lithology has the highest impact in the landslide susceptibility, followed by altitude, aspect, slope, and land use, while others are less significant in the landslide susceptibility of the region. It is seen that slope in the case of curvature, the concave slope is most susceptible to landslides, followed by convex slope. The slopes ranging in altitude between 350 and 500 m have the highest (Pij) value of 1.4, followed by 500–650 m (1.15), 200–350 m (1.13), and 650–800 m (1.02) intervals. It is seen that the landslide density increases from 200 to 500 m, and it gradually decreases from 500 m upward. From the analysis of (Pij) value of geology, it is seen that the Middle Siwaliks, Lower Siwaliks, alluvial deposits, Purebesi Quartzite followed by amphibolites are more susceptible to landslides. In the case of distance from faults, 400–500 m range has the highest Pij value (1.28) followed by 100–200 m (1.26), 300–400 m (1.13), and 200–300 m (1.09). The distance from rivers shows that the Pij value decreases as the distance from river increases. From this, it is clear that the bank erosion is one of the main triggering factors. Most of the landslides are located at a distance of 200–250 m from the road section as the values of (Pij) is highest (0.2) here. It decreases with both the increase and decrease of distance from the road. In the case of TWI (Pij), the value decreases with increasing TWI, it is highest (0.42) for class 0–8. This shows that TWI strongly affects the landslide

occurrence. In the case of SPI, class 150–300 has the highest (Pij) value, while for STI, the range between 80 and120 has the highest (Pij) value, indicating that this range is most susceptible to landsliding. The cultivation land has the highest (Pij) value of 1.57 and is the main land use type that is most susceptible for landsliding.

From the W_j value, it is seen that geology has the highest impact in the landslide susceptibility, followed by altitude, aspect, slope and land use, while the other have very minor role. From the calculated (P_{ij}) it is seen that slope ranging in between 35–45 are highly prone to landslide followed by slope class 25–35. In the case of aspect SE facing slope followed by S facing, E facing and SW facing slope are susceptible landslide. The slopes ranging in altitude 350–500 m have the highest (P_{ij}) value, followed by 500–650 m, 200–350 m and 650 m–800 m. From this it is seen that the landslide density increases form 200 m to 500 m and it gradually decreases form 500 m upward. By the analysis of (P_{ij}) value of geology, it is seen that Middle Siwaliks, Lower Siwaliks, Terrace deposits, Purebesi Quartzite, Amphibolite followed by Dhading Dolomite more susceptible to landslide. In the case of distance from fault, 100–200 m range has the highest P_{ij} value (0.2) followed by 400–500 m and 200–300 m. This shows that the faults have little impact in landslide generation in this study area. The distance form river show that the P_{ij} value decreases as the distance from river increases. From this it becomes clear that the bank erosion is the main reason for the landslides. Most of the landslides are located at a distance of 200–250 m form the road section as the values of (P_{ij}) is highest (0.2) here. It decreases with both the increase and decrease of distance from the road. In the case of TWI (P_{ij}) value decreases with increase in TWI value, it is highest (0.42) for class 0–8. This shows that TWI strongly affects the landslide occurrence. In the case of SPI class 150–300 has the highest (P_{ij}) value, while in the

case of STI, the range in between 80–120 has the highest (P_{ij}) value, indicating that this range is most susceptible to landslides. The cultivation land followed by grass land and orchard show high susceptible to landslides as they have higher (P_{ij}) value. In the case of curvature, the concave slope is most susceptible to landslides, followed by convex slope.

7.3 Logistic regression Model

The resulting beta (β) coefficients of each independent variable in the logistic regression equation are given in Table 3. Based on the obtained result, Eq. 15 can be rewritten as

$$\begin{aligned} z = {} & (0.0214 \times SLOPE) + ASPECT + (0.0221 \times CURVATURE) + (0.038 \times SPI) \\ & + (-0.2831 \times TWI) + LITHOLOGY + LAND\ USE \\ & + (-0.000041 \times DISTANCE\ FROM\ FAULT) \\ & + (-0.00038 \times DISTANCE\ FORM\ ROAD) \\ & + (-0.0004 \times DISTANCE\ FORM\ RIVER) - 18.991 \end{aligned} \tag{15}$$

Finally, landslide susceptibility index (LSI) map is obtained by using the raster calculator in ArcGIS 9.3 (Fig. 7).

From the analysis of logistic regression coefficients, it is seen that slope angle, curvature, and SPI have prominent role in the landslide susceptibility of the area, as they all have positive β value. Also, it is seen that SPI has highest β coefficient (0.038), followed by curvature (0.0221) and slope (0.0214). Distance from fault, road, river, and TWI has negative effect in landslide formation as they all have negative β coefficient and hence are considered to be less significant in landslide formation on the road section. In the case of aspect, the slope trending toward east (β = 0.8658), south (β = 0.5532), southeast (β = 0.3029), and west (β = 0.1169) has high probability of landslide susceptibility as they have positive b coefficient. As far as the geology is concerned,

the Middle Siwaliks (β = 2.369) are most susceptible to sliding. Alluvial deposits (β = 0.606), consisting of loose sediments, also show a higher susceptibility. The Lower Siwaliks (β = 0.591) are also highly prone to landsliding; the Benighat Slates (β = 0.369), Nourpul Formation (β = 0.294), and Amphibolites (β = 0.127) all have positive b coefficient and hence are more susceptible to landsliding than the rest. In the case of land use, barren land (β = 14.447), cultivated land (β = 13.445), orchard (β = 13.108), followed by bush (β = 12.814), and grassland (β = 12.954) have the susceptibility levels in decreasing order, while the remaining land use types does not have any role in landslide susceptibility of the region.

7.4 Validation of the landslide susceptibility maps

The landslide susceptibility maps derived by three models were tested using the landslide data sets that were used for model building process as well as from those that were not used in model building process. For this, the total landslides observed in the study area were split into 2 parts, 241 (75 %) was randomly selected from the total 321 landslides as the training data and the remaining 80 (25 %) landslides are kept for validation propose. Spatial effectiveness of these susceptibility maps was checked by receiver operating characteristics (ROC).

The ROC curve is a useful method for representing the quality of deterministic and probabilistic detection and forecast systems (Swets 1988). The ROC can be represented equivalently by plotting the fraction of true positives out of the positives versus the fraction of false positives out of the negatives, for a binary classifier system as its discrimination threshold is varied (Table 4). By tradition, the plot shows the false-positive rate (1 spec- ificity) on the x-axis (Eq. 16) and the true-positive rate (the sensitivity or 1—the false- negative rate) on the y-axis (Eq. 17).

$$X = 1 - specifity = 1 - [\frac{TN}{(TN + FP)}] \qquad (16)$$

$$Y = sensitivity = [\frac{TN}{(Tp + FN)}] \qquad (17)$$

The area under the ROC curve (AUC) characterizes the quality of a forecast system by describing the system's ability to predict correctly the occurrence or non-occurrence of predefined 'events'. The model with higher AUC is considered to be the best. If the area under the ROC curve (AUC) is close to 1, the result of the test is excellent. On the other hand, if the model does not predict well, then this value will be close to 0.5. Both the success rate and prediction rate of the models were used for assessing the prediction capability of the models.

The success rate results were obtained by comparing the landslide training data with the susceptibility maps (Fig. 8a). From the figure, it is seen that the index of entropy model (IOE) has the highest area under the curve (AUC) value (0.8915), followed by logistic regression model (0.8910) and certainty factor model (0.8721). Since the success rate method used the training landslide data that have already been used for building the landslide models, the success rate is not a suitable method for assessing the prediction capability of the models (Bui et al. 2011). However, this method is useful to know the performance of the models. Thus, the validations of the models were done by using the prediction rate curve. The prediction rate explains how well the model and predictor

8 Conclusions

Since landslides pose a serious threat to the life and property, their susceptibility mapping can be one of the preliminary steps toward minimizing the damages incurred by them. A landslide susceptibility map divides an area into various categories that range from stable to unstable ones. In this research, two bivariate models (i.e., certainty factor and index of entropy models) and one

multivariate model (i.e., logistic regression) were used for identifying the areas susceptible to landsliding at Mugling–Narayanghat road and its surrounding areas.

For this purpose, twelve landslide conditioning factors (i.e., slope gradient; slope aspect; altitude; plan curvature; lithology; land use; distance from faults, rivers and roads; topographic wetness index(TWI); stream power index(SPI);and sediment transport index (STI)) were used. A landslide inventory map was prepared using aerial photographs, satellite images, and extensive field survey. In this process, a total of 321 landslides were identified and mapped. Out of which, 241 (75 %) were randomly selected for generating a model and the remaining 80 (25 %) were used for validation proposes. The ROC plots showed that the susceptibility map produced using the index of entropy model has the highest perdition accuracy (90.16 %), followed by the logistic regression model (86.29 %) and the certainty factor model (83.57 %). Success rate curve also gives similar result, with index of entropy model (IOE) the highest (AUC) value (0.8915), followed by logistic regression model (0.8910)and certainty factor model (0.8721).This shows that all the models employed in this study showed reasonably good accuracy in predicting the landslide susceptibility of Mugling–Narayanghat road section. The increasing population pressure has forced people to concentrate their activities on steep mountain slopes. Thus, to safeguard the life and property from landslides, the susceptibility maps can be used as basic tools in land management and planning future construction projects in this area. While the low susceptibility zones are relatively safe for the development of infrastructures, the high and very high susceptibility zones require further engineering geological and geotechnical considerations.

Acknowledgments

The authors are thankful to anonymous reviewers for their valuable comments which were very useful in bringing the manuscript into its present form. The authors also express their gratitude to

MEXT (Ministry of Education, Culture, Sports, Science and Technology, Japan) for funding for the present study. Mr. Binod Regmi, Mr. Ishan Basyal and Miss. Shristi Bhusal are sincerely acknowledged for their great help during the field work and in writing this manuscript. This research was supported by the BK21 and the Energy Resources and Environmental Geology Team, Kyungpook National University, Republic of Korea.

References

Adhikari TL (2009) Disaster mitigation works along Narayanghat Mugling Highway. In: International seminar on hazard management for sustainable development

Ahmad R, Joshi MN (2010) Assessment of landslide susceptibility on land degradation processes in Cha- moli and surrounding area using RS and GIS technique. Int Geoinf Res Dev J 1(3)

Akgűn A, Dag S, Bulut F (2008) Landslide susceptibility mapping for a landslide prone area (Findikli, NE of Turkey) by likelihood-frequency ratio and weighted linear combination models. Environ Geol 54:1127–1143

Akgűn A, Kincal C, Pradhan B (2011) Application of remote sensing data and GIS for landslide risk assessment as an environmental threat to Izmir city (west Turkey). Environ Monit Assess. doi: 10.1007/s10661-011-2352-8 (Article online first available)

Akgűn A, Sezer EA, Nefeslioglu HA, Gokceoglu C, Pradhan B (2012) An easy-to-use MATLAB program (MamLand) for the assessment of landslide susceptibility using a Mamdani fuzzy algorithm. Comput Geosci 38(1):23–34

Aleotti P, Chowdhury R (1999) Landslide hazard assessment: summary review and new perspectives. Bull Eng Geol Environ 58:21–44

Althuwaynee OF, Pradhan B, Lee S (2012) Application of an evidential belief function model in landslide susceptibility mapping. Comput Geosci 44:120–135. doi:10.1016/j.cageo.2012.3

Atkinson PM, Massari R (1998) Generalized linear modeling of susceptibility to landsliding in the central Apennines, Italy. Comput Geosci 24:373–385

Ayalew L, Yamagishi H (2005) The application of GIS-based logistic regression for landslide susceptibility mapping in the Kakuda-Yahiko Mountains, Central Japan. Geomorphology 65(1–2):15–31

Ayalew L, Yamagishi H, Ugawa N (2004) Landslide susceptibility mapping using GIS based weighted linear combination, the case in Tsugawa area of Agano River, Niigata Prefecture, Japan. Landslides 1(1):73–81

Bednarik M, Magulova B, Matys M, Marschalko M (2010) Landslide susceptibility assessment of the Kralovany–Liptovsky Mikulas railway case study. Phys Chem Earth Parts A/B/C 35(3–5):162–171

Bednarik M, Yilmaz I, Marschalko M (2012) Landslide hazard and risk assessment: a case study from the Hlohovec–Sered' landslide area in south-west Slovakia. Nat Hazards. doi:10.1007/s11069-012-0257-7

Bonham-Carter GF (1991) Integration of geoscientific data using GIS. In: Goodchild MF, Rhind DW, Maguire DJ (eds) Geographic information systems: principle and applications. Longdom, London, pp 171–184

Brabb EE (1984) Innovative approaches to landslide hazard mapping. In: Proceedings 4th international symposium on landslides, Toronto, vol 1, pp 307–324

Brenning A (2005) Spatial prediction models for landslide hazards: review, comparison and evaluation. Nat Hazard Earth Syst 5:853–862

Brunsden D, Doornkamp JC, Fookes PG, Jones DKC, Kelly JMH (1975) Large-scale geotechnical mapping and highway engineering design. Q J Eng Geol 8:227–253

Bui DT, Pradhan B, Lofman O, Revhaug I, Dick OB (2011) Landslide susceptibility mapping at Hoa Binh province (Vietnam) using an adaptive neuro fuzzy inference system and GIS. Comput Geosci (Article on-line first available). doi:10.1016/j.cageo.2011.10.031

Bui DT, Pradhan B, Lofman O, Revhaug I, Dick OB (2012a) Landslide susceptibility assessment in the Hoa Binh province of Vietnam using Artificial Neural Network. Geomorphology. doi:10.1016/ j.geomorph.2012.04.023 (Article online first available)

Bui DT, Pradhan B, Lofman O, Revhaug I, Dick OB (2012b) Spatial prediction of landslide hazards in Vietnam: a comparative assessment of the efficacy of evidential belief functions and fuzzy logic models. Catena 96:28–40

Bui DT, Pradhan B, Lofman O, Revhaug I (2012c) Landslide susceptibility assessment in Vietnam using support vector machines, decision tree and Naïve Bayes models. Math Probl Eng 2012:1–26. doi: 10.1155/2012/974638

Can T, Nefeslioglu HA, Gokceoglu C, Sonmez H, Duman TY (2005) Susceptibility assessments of shallow earthflows triggered by heavy rainfall at three subcatchments by logistic regression analyses. Geo- morphology 72(1–4):250–271

Choi J, Oh HJ, Lee HJ, Lee C, Lee S (2012) Combining landslide susceptibility maps obtained from frequency ratio, logistic regression, and artificial neural network models using ASTER images and GIS. Eng Geol 124:12–23

Chung CJ, Fabbri AG (1999) Probabilistic prediction models for landslide hazard mapping. Photogramm Eng Rem S 65(12):1389–1399

Chung CJ, Fabbri AG (2003) Validation of spatial prediction models for landslide hazard mapping. Nat Hazards 30:451–472

Chung CJ, Fabbri AG (2005) Systematic procedures of landslide hazard mapping for risk assessment using spatial prediction models. In: Glade T, Anderson MG, Crozier MJ (eds) Landslide hazard and risk. Wiley, New York, pp 139–177

Constantin M, Bednarik M, Jurchescu MC, Vlaicu M (2011) Landslide susceptibility assessment using the bivariate statistical analysis and the index of entropy in the Sibiciu Basin (Romania). Environ Earth Sci 63:397–406

Dahal RK, Hasegawa S (2008) Representative rainfall thresholds for landslides in the Nepal Himalaya. Geomorphology 100:429–443

Dahal RK, Hasegawa S, Nonomura A, Yamanaka M, Dhakal S, Paudyal P (2008) Predictive modelling of rainfall-induced landslide hazard in the Lesser Himalaya of Nepal based on weights-of evidence. Geomorphology 102(3–4):496–510

Dahal RK, Hasegawa S, Bhandary NP, Poudel PP, Nonomurac A, Yatabe Y (2012) A replication of landslide hazard mapping at catchment scale. Geomat Nat Hazards Risk. doi:10.1080/19475705.2011.629007

Deoja B, Dhital MR, Thapa B, Wagner A (1991) Mountain risk engineering handbook. In: ICIMOD, Kathmandu, 857 pp

Dhakal AS, Amada T, Aniya M (2000) Landslide hazard mapping and its evaluation using GIS: an investigation of sampling schemes for a grid-cell based quantitative method. Photogramm Eng Remote S 66(8):981–989

Dhital MR (2000) An overview of landslide hazard mapping and rating systems in Nepal. J Nepal Geol Soc 22:533–538

Dhital MR, Upreti BN, Dangol V, Bhandari AN, Bhattarai TN (1991) Geological engineering methods applied in mountain road survey: an example from Baitadi-Darchula Road Project (Nepal). J Nepal Geol Soc 7:49–67

Dhital MR, Shrestha R, Ghimire M, Shrestha GB, Tripathi D (2006) Hydrological hazard mapping in Rupandehi district, West Nepal. J Nepal Geol Soc 31:59–66

DoR/USAID (1986) Rapti road assessment study, engineering studies, final technical report (Vol. II). Unpublished report submitted to the Department of Roads (DoR) and the USAID by Luis Berger International Inc. and East Consult (P) Ltd (unpubl)

DPTC (Water Induced Disaster Prevention Technical Centre) (1996) A technical guideline on landslide prevention works. Government of Nepal, Ministry of Water Resources, Water Induced Disaster Prevention Technical Centre, Pulchowk, Lalitpur, 50 pp

DWIDP (2009) The study on disaster risk management for Narayanghar–Mugling Highway. Unpublished report

Einstein HH (1988) Special lecture: landslides risk assessment procedure. In: Proceedings of 5th symposium on landslides, Lausanne, vol 2, pp 1075–1090

Ercanoglu M, Gokceoglu C (2002) Assessment of landslide susceptibility for a landslide prone area (north of Yenice, NW Turkye) by fuzzy approach. Environ Geol 41:720–730

Ercanoglu M, Gokceoglu C (2004) Use of fuzzy relations to produce landslide susceptibility map of a landslide prone area (West Black Sea Region, Turkey). Eng Geol 75:229–250

Ercanoglu M, Gokceoglu C, van Asch TWJ (2004) Landslide susceptibility zoning north of Yenice (NW Turkey) by multivariate statistical techniques. Nat Hazards 32:1–23

Erener A, Dűzgűn HSB (2010) Improvement of statistical landslide susceptibility mapping by using spatial and global regression methods in the case of More and Romsdal (Norway). Landslides 7(1):55–68

Ganser A (1964) Geology of the Himalaya. Inter Science John Wiley, London

Gerrard J (1994) The landslide hazard in the Himalayas: geological control and human action. Geomorphology 10:221–230

Gerrard AJ, Gardner RAM (2000a) The role of landsliding in shaping the landscape of the middle hills, Nepal. Z Geomorphol Suppl Bd 122:47–62

Gerrard AJ, Gardner RAM (2000b) The nature and management implications of landsliding on irrigated terraces in the Middle Hills of Nepal. Int J Sust Dev World 7:229–236

Gökçeolu C, Sonmez H, Nefeslioglu HA, Duman TY, Can T (2005) The 17 March 2005 Kuzulu landslide (Sivas, Turkey) and landslide-susceptibility map of its near vicinity. Eng Geol 81:65–83

Gorum T, Gonencgil B, Gökçeolu C, Nefeslioglu HA (2008) Implementation of reconstructed geomor- phologic units in landslide susceptibility mapping: the Melen Gorge (NW Turkey). Nat Hazards 46(3):323–351

Guzzetti F, Carrara A, Cardinali M, Reichenbach P (1999) Landslide hazard evaluation: a review of current techniques and their application in a multi-scale study, Central Italy. Geomorphology 31:181–216

Guzzetti F, Reichenbach P, Cardinali M, Galli M, Ardizzone F (2005) Probabilistic landslide hazard assessment at the basin scale. Geomorphology 72:272–299

Hagen T (1969) Report on the geological survey of Nepal preliminary reconnaissance: Zürich, Me´moires de la soc. Helve´tique des sci. naturelles, 185pp

Hasegawa S, Dahal RK, Yamanaka M, Bhandari NP, Yatabe R, Inagaki H (2009) Causes of large landslides in the Lesser Himalaya of central Nepal. Environ Geol 57:1423–1434

Ives JD, Messerli B (1981) Mountain hazards mapping in Nepal; introduction to an applied mountain research project, vol 1. Mountain Research and Development, University of California Press, Berkeley, pp 223–230

Jia N, Xie M, Mitani Y, Ikemi H, Djamaluddin I (2010) A GIS-based spatial data processing system for slope monitoring. Int Geoinf Res Dev J 1(4)

Kanungo DP, Arora MK, Gupta RP, Sarkar S (2008) Landslide risk assessment using danger pixel and fuzzy concepts in Darjeeling Himalayas. Landslides 5:407–416

Kanungo DP, Sarkar S, Sharma S (2011) Combining neural network with fuzzy, certainty factor and likelihood ratio concepts for spatial prediction of landslides. Nat Hazards 59:1491–1512

Karimi Nasab S, Ranjbar H, Akbar S (2010) Susceptibility assessment of the terrain for slope failure using remote sensing and GIS, a case study of Maskoon area, Iran. Int Geoinf Res Dev J 1(3)

Kojan E (1978) Report on landslide problems, western hill road project, Godavari to Dandeldhura, Nepal. Unpublished Report, USAID

Laban P (1979) Landslide occurrence in Nepal. HMG/FAO and UNDP, Ministry of Forest, Department of Soil Conservation, Integrated Watershed Management, Kathmandu, 27 pp

Lee S (2007) Landslide susceptibility mapping using an artificial neural network in the Gangneung area, Korea. Int J Remote Sens 28:4763–4783

Lee S, Min K (2001) Statistical analyses of landslide susceptibility at Yongin, Korea. Environ Geol 40:1095–1113

Lee S, Pradhan B (2006) Probabilistic landslide hazards and risk mapping on Penang Island, Malaysia. J Earth Sys Sci 115(6):661–667

Lee S, Pradhan B (2007) Landslide hazard mapping at Selangor, Malaysia using frequency ratio and logistic regression models. Landslides 4(1):33–41

Lee S, Ryu JH, Won JS, Park HJ (2004) Determination and application of the weights for landslide susceptibility mapping: using an artificial neural network. Eng Geol 71:289–302

Lee S, Ryu JH, Kim IS (2007) Landslide susceptibility analysis and its verification using likelihood ratio, logistic regression, and artificial neural network models: case study of Youngin, Korea. Landslides 4:327–338

Magliulo P, Lisio AD, Russo F, Zelano A (2008) Geomorphology and landslide susceptibility assessment using GIS and bivariate statistics: a case study in southern Italy. Nat Hazards 47(3):411–435

Moore ID, Grayson RB (1991) Terrain-based catchment partitioning and runoff prediction using vector elevation data. Water Resour Res 27(6):1171–1191

Nefeslioglu HA, Gokceoglu C, Sonmez H (2008) An assessment on the use of logistic regression and artificial neural networks with different sampling strategies for the preparation of landslide suscepti- bility maps. Eng Geol 97(3–4):171–191

Nefeslioglu HA, Sezer E, Gokceoglu C, Bozkir A, Duman T (2010) Assessment of landslide susceptibility by decision trees in the metropolitan area of Istanbul, Turkey. Math Probl Eng, Article ID 901095

Neuhäuser B, Terhorst B (2007) Landslide susceptibility assessment using “weights-of-evidence” applied to a study area at the Jurassic escarpment (SW- Germany). Geomorphology 86:12–24

Oh HJ, Pradhan B (2011) Application of a neuro-fuzzy model to landslide-susceptibility mapping for shallow landslides in a tropical hilly area. Comput Geosci 7(9):1264–1276. doi:10.1016/j.cageo. 2010.10.012

Oh HJ, Park NW, Lee SS, Lee S (2011) Extraction of landslide-related factors from ASTER imagery and its application to landslide susceptibility mapping. Int J Remote Sens 33(10):3211–3231

Pareek N, Sharma ML, Arora MK (2010) Impact of seismic factors on landslide susceptibility zonation: a case study in part of Indian Himalayas. Landslides 7(2):191–201

Petley DN, Hearn GJ, Hart A, Rosser NJ, Dunning SA, Oven K, Mitchell WA (2006) Trends in landslide occurrence in Nepal. Nat Hazards 43:23–44

Poudyal CP, Chang C, Oh HJ, Lee S (2010) Landslide susceptibility maps comparing frequency ratio and artificial neural networks: a case study from the Nepal Himalaya. Environ Earth Sci 61:1049–1064

Pourghasemi HR, Pradhan B, Gokceoglu C, Mohammadi M, Moradi HR (2012a) Application of weights-of- evidence and certainty factor models and their comparison in landslide susceptibility mapping at Haraz watershed, Iran. Arab J Geosci. doi:10.1007/s12517-012-0532-7

Pourghasemi HR, Pradhan B, Gokceoglu C, Deylami Moezzi K (2012b) A comparative assessment of prediction capabilities of Dempster-Shafer and Weights-of-evidence models in landslide susceptibility mapping using GIS, Geomatics. Nat Hazards Risk. doi:10.1080/19475705.2012.662915

Pourghasemi HR, Pradhan B, Gokceoglu C (2012c) Application of fuzzy logic and analytical hierarchy process (AHP) to landslide susceptibility mapping at Haraz watershed, Iran. Nat Hazards. doi: 10.1007/s11069-012-0217-2

Pourghasemi HR, Gokceoglu C, Pradhan B, Deylami Moezzi K (2012d) Landslide susceptibility mapping using a spatial multi criteria evaluation model at Haraz Watershed, Iran. In: Pradhan B, Buchroithner M (eds) Terrigenous mass movements. Springer, Berlin, pp 23–49, doi: 10.1007/978-3-642-25495-6-2

Pourghasemi HR, Mohammady M, Pradhan B (2012e) Landslide susceptibility mapping using index of entropy and conditional probability models in GIS: Safarood Basin, Iran. Catena 97:71–84. doi: 10.1016/j.catena.2012.05.005

Pradhan B (2010a) Remote sensing and GIS-based landslide hazard analysis and cross-validation using multivariate logistic regression model on three test areas in Malaysia. Adv Space Res 45(10): 1244–1256

Pradhan B (2010b) Application of an advanced fuzzy logic model for landslide susceptibility analysis. Int J Comput Int Sys 3(3):370–381

Pradhan B (2010c) Landslide susceptibility mapping of a catchment area using frequency ratio, fuzzy logic and multivariate logistic regression approaches. J Indian Soc Remote Sens 38(2):301–320. doi: 10.1007/s12524-010-0020-z

Pradhan B (2011a) Manifestation of an advanced fuzzy logic model coupled with geoinformation techniques coupled with geoinformation techniques for landslide susceptibility analysis. Environ Ecol Stat 18(3):471–493. doi:10.1007/s10651-010-0147-7

Pradhan B (2011b) Use of GIS-based fuzzy logic relations and its cross application to produce landslide susceptibility maps in three test areas in Malaysia. Environ Earth Sci 63(2):329–349

Pradhan B, Buchroithner MF (2010) Comparison and validation of landslide susceptibility maps using an artificial neural network model for three test areas in Malaysia. Environ Eng Geosci 16(2):107–126

Pradhan B, Lee S (2009) Landslide risk analysis using artificial neural network model focusing on different training sites. Int J Phys Sci 3(11):1–15

Pradhan B, Lee S (2010a) Delineation of landslide hazard areas using frequency ratio, logistic regression and artificial neural network model at Penang Island, Malaysia. Environ Earth Sci 60:1037–1054

Pradhan B, Lee S (2010b) Regional landslide susceptibility analysis using back propagation neural network model at Cameron Highland, Malaysia. Landslides 7:13–30

Pradhan B, Lee S (2010c) Landslide susceptibility assessment and factor effect analysis: back propagation artificial neural networks and their comparison with frequency ratio and bivariate logistic regression modelling. Environ Model Softw 25(6):747–759

Pradhan B, Pirasteh S (2010) Comparison between prediction capabilities of neural network and fuzzy logic techniques for landslide susceptibility mapping. Disaster Adv 3(2):26–34

Pradhan B, Youssef AM (2010) Manifestation of remote sensing data and GIS on landslide hazard analysis using spatial-based statistical models. Arab J Geosci 3(3):319–326

Pradhan B, Singh RP, Buchroithner MF (2006) Estimation of stress and its use in evaluation of landslide prone regions using remote sensing data. Adv Space Res 37:698–709

Pradhan B, Lee S, Mansor S, Buchroithner MF, Jallaluddin N, Khujaimah Z (2008) Utilization of optical remote sensing data and geographic information system tools for regional landslide hazard analysis by using binomial logistic regression model. Appl Remote Sens 2:1–11

Pradhan B, Lee S, Buchroithner MB (2009) Use of geospatial data for the development of fuzzy algebraic operators to landslide hazard mapping: a case study in Malaysia. Appl Geomat 1:3–15

Pradhan B, Sezer EA, Gokceoglu C, Buchroithner MF (2010a) Landslide susceptibility mapping by neuro- fuzzy approach in a landslide-prone area (Cameron Highlands, Malaysia). IEEE Trans Geosci Remote 48(12):4164–4177

Pradhan B, Youssef AM, Varathrajoo R (2010b) Approaches for delineating landslide hazard areas using different training sites in an advanced artificial neural network model. Geo-Spat Inf Sci 13(2):93–102

Pradhan B, Lee S, Buchroithner MF (2010c) Remote sensing and GIS based landslide susceptibility analysis and its cross-validation in three test areas using a frequency ratio model. Photogramm Fernerkun 2010(1):17–32. doi:10.1127/14328364/2010/0037

Pradhan B, Oh HJ, Buchroithner M (2010d) Weights-of-evidence model applied to landslide susceptibility mapping in a tropical hilly area. Geomatics Nat Hazards Risk 1(3):199–223. doi:10.1080/19475705. 2010.498151

Pradhan B, Mansor S, Pirasteh S, Buchroithner M (2011) Landslide hazard and risk analyses at a landslide prone catchment area using statistical based geospatial model. Int J Remote Sens 32(14):4075–4087. doi:10.1080/01431161.2010.484433

Pradhan B, Chaudhari A, Adinarayana J, Buchroithner MF (2012) Soil erosion assessment and its corre- lation with landslide events using remote sensing data and GIS: a case study at Penang Island, Malaysia. Environ Monit Assess 184(2):715–727

Rajbhandari PCL, Alam BM, Akther MS (2002) Application of GIS (Geographic Information System) for landslide hazard zonation and mapping disaster prone area: a study of Kulekhani Watershed, Nepal. Plan plus 1(1):117–123

Regmi NR, Giardino JR, Vitek JD (2010a) Modeling susceptibility to landslides using the weight of evidence approach: Western Colorado, USA. Geomorphology 115:172–187

Regmi NR, Giardino JR, Vitek JD (2010b) Assessing susceptibility to landslides: using models to under- stand observed changes in slopes. Geomorphology 112:25–38

Regmi AD, Yoshida K, Dhital MR, Devkota K (2012) Effect of rock weathering, clay mineralogy, and geological structures in the formation of large landslide, a case study from Dumre Besei landslide, Lesser Himalaya Nepal. Landslides. doi:10.1007/s10346-011-0311-7

Saha AK, Gupta RP, Sarkar I, Arora KM, Csaplovics E (2005) An approach for GIS-based statistical landslide susceptibility zonation with a case study in the Himalayas. Landslides 2(1):61–69

Saito H, Nakayama D, Matsuyama H (2009) Comparison of landslide susceptibility based on a decision-tree model and actual landslide occurrence: the Akaishi Mountains, Japan. Geomorphology 109:108–121

Sezer EA, Pradhan B, Gokceoglu C (2011) Manifestation of an adaptive neuro-fuzzy model on landslide susceptibility mapping: Klang valley, Malaysia. Expert Syst Appl 38(7):8208–8219

Shroder JF, Bishop MP (1998) Mass movements in the Himalaya: new insights and research directions. Geomorphology 26:13–36

Soeters R, van Westen CJ (1996) Slope stability recognition analysis and zonation. In: Turner AK, Schuster RL (eds) Landslides: investigation and mitigation, transportation research board special report 247. National Academy Press, Washington, pp 129–177

Stöcklin J (1980) Geology of Nepal and its regional frame. J Geol Soc Lond 137:1–34

Stöcklin J, Bhattarai KD (1978) Geology of the Kathmandu area and central Mahabharat range. Nepal Himalaya. Report of Department of Mines and Geology/UNDP (unpublished), 86 pp

Swets JA (1988) Measuring the accuracy of diagnostic systems. Science 240:1285–1293

Tunusluoglu MC, Gokceoglu C, Nefeslioglu HA, Sonmez H (2008) Extraction of potential debris source areas by logistic regression technique: a case study from Barla, Besparmak and Kapi mountains (NW Taurids, Turkey). Environ Geol 54:9–22

Vahidnia MH, Alesheikh AA, Alimohammadi A, Hosseinali F (2010) A GIS-based neuro-fuzzy procedure for integrating knowledge and data in landslide susceptibility mapping. Comput Geosci 36(9): 1101–1114

Van Westen CJ (2004) Geo-information tools for landslide risk assessment: an overview of recent devel- opments. In: Lacerda W, Ehrlich M, Fontoura SAB, Sayao ASF (eds) Landslides: evaluation and stabilization. Taylor and Francis, Balkema, pp 39–57

Van Westen CJ, Rengers N, Soeters R (2003) Use of geomorphological information in indirect landslide susceptibility assessment. Nat Hazards 30:399–419

Varnes DJ (1984) Commission on landslides and other mass movements: landslide hazard zonation: a review of principles and practice. UNESCO Press, Paris 63 pp

Vlcko J, Wagner P, Rychlikova Z (1980) Evaluation of regional slope stability. Mineralia Slovaca 12(3):275–283 Wagner A (1981) Rock structure and slope stability study of Waling area, central west Nepal. J Nepal Geol Soc 1(2):37–43

Wan S (2009) A spatial decision support system for extracting the core factors and thresholds for landslide susceptibility map. Eng Geol 108:237–251

Wang HB, Wu SR, Shi JS, Li B (2011) Qualitative hazard and risk assessment of landslides: a practical framework for a case study in China. Nat Hazards. doi:10.1007/s11069-011-0008-1

Wieczorek GF (1984) Preparing a detailed landslide-inventory map for hazard evaluation and reduction. As Eng Geol Bull 21(3):337–342

Xu C, Xu X, Lee YH, Tan X, Yu G, Dai F (2012) The 2010 Yushu earthquake triggered landslide hazard mapping using GIS and weight of evidence modeling. Environ Earth Sci. doi:10.1007/s12665- 012-1624-0

Yilmaz I (2009a) A case study from Koyulhisar (Sivas-Turkey) for landslide susceptibility mapping by artificial neural networks. Bull Eng Geol Environ 68:297–306

Yilmaz I (2009b) Landslide susceptibility mapping using frequency ratio, logistic regression, artificial neural networks and their comparison: a case study from Kat landslides (Tokat-Turkey). Comput Geosci 35:1125–1138

Yilmaz I (2010a) Comparison of landslide susceptibility mapping methodologies for Koyulhisar, Turkey: conditional probability, logistic regression, artificial neural networks, and support vector machine. Environ Earth Sci 61:821–836

Yilmaz I (2010b) The effect of the sampling strategies on the landslide susceptibility mapping by condi- tional probability and artificial neural networks. Environ Earth Sci 60:505–519

Zarea M, Pourghasemi HR, Vafakhah M, Pradhan B (2012) Landslide susceptibility mapping at Vaz watershed (Iran) using an artificial neural network model: a comparison between multi-layer percep- tron (MLP) and radial basic function (RBF) algorithms. Arab J Geosci. doi:10.1007/s12517-012- 0610-x (Article online first available)

Table 1 Spatial relationship between each landslide conditioning factor and landslide by frequency ratio and certainty factor

Factor	Class	No. of pixels in domine	Percentage of domine (a)	No. of landslide	Percentage of landslides (b)	Certainty Factor
Slope degree	0-15°	22111	13.76	6	2.49	-0.82
	15-25°	30542	19.01	45	18.67	-0.02
	25-35°	42515	26.47	86	35.68	0.26
	35-45°	40693	25.33	88	36.51	0.31
	>45°	24776	15.42	16	6.64	-0.57
Slope aspect	Flat	1201	0.75	0	0	-1
	North	29104	18.12	31	12.86	-0.29
	Northeast	18906	11.77	20	8.3	-0.3
	East	12363	7.7	25	10.37	0.26
	Southeast	11936	7.43	31	12.86	0.42
	South	18154	11.3	43	17.84	0.37
	Southwest	21037	13.1	36	14.94	0.12
	West	23680	14.74	29	12.03	-0.18
	Northwest	24125	15.02	26	10.79	-0.28
Plan Curvature (100/m)	Concave	73478	45.74	114	47.3	0.03
	Flat	2127	1.32	0	0	-1
	Convex	84894	52.85	127	52.7	-0.003
Elevation(m)	<350	25421	15.83	43	17.84	0.11
	350-501	34691	21.6	73	30.29	0.29
	501-650	27266	16.97	47	19.5	0.13
	651-800	25533	15.89	39	16.18	0.02
	800-950	24907	15.51	19	7.88	-0.49
	951-1100	19790	12.32	20	8.3	-0.33
	1101-1250	2357	1.47	0	0	-1
	>1250	672	0.42	0	0	-1
SPI	0-150	14196	8.84	8	3.32	-0.62
	150-300	19750	12.29	39	16.18	0.24
	300-450	14807	9.22	21	8.72	-0.06
	>450	111884	69.65	173	71.78	0.03
TWI	<8	86989	54.15	148	61.41	0.12
	10	51763	32.22	73	30.29	-0.06
	>10	21885	13.62	20	8.3	-0.39
STI	0-40	22258	13.86	17	7.05	-0.49
	40-80	30532	19.01	55	22.82	0.17
	80-120	25488	15.87	51	21.16	0.25
	>120	82359	51.27	118	48.96	-0.05
Land Use	Barren	220	0.14	0	0	-1
	Bush	38983	24.27	40	16.6	-0.32
	Cultivation	49758	30.98	117	48.55	0.36
	Cutting	128	0.08	0	0	-1
	Forest	994	0.62	0	0	-1
	Grass	68712	42.77	82	34.02	-0.2
	Orchard	1451	0.9	2	0.83	-0.08
	River	255	0.16	0	0	-1
	Sand	5	0.003	0	0	-1
Lithology	Amphibolite	617	0.38	1	0.415	0.07
	Benighat Slate	16221	10.1	24	9.96	-0.01
	Dandagaun Formation	849	0.53	0	0	-1
	Dhading Dolomite	26709	16.63	26	10.79	-0.35
	Fagfog Quartzite	961	0.6	2	0.83	0.28
	Kuncha Formation	1988	1.24	1	0.41	-0.66
	Lower Siwaliks	2488	1.55	10	4.15	0.63
	Middle Siwaliks	65	0.04	1	0.41	0.9
	Nourpul Formation	82099	51.11	122	50.62	-0.01
	Purebesi Quartzite	1303	0.81	1	0.41	-0.49
	Terrace Deposits	27206	16.94	55	22.82	0.26
Distance from Faults (m)	0-100	25436	15.83	33	13.69	-0.14
	100-200	22302	13.88	42	17.43	0.2
	200-300	20801	12.95	34	14.11	0.08
	300-400	17733	11.04	30	12.45	0.11
	400-500	15127	9.42	29	12.03	0.22
	>500	59107	36.8	73	30.29	-0.18
Distance from rivers (m)	0-50	54983	34.23	100	41.49	0.17
	50-100	38565	24.01	58	24.07	0.002
	100-150	26264	16.35	39	16.18	-0.01
	150-200	17252	10.74	23	9.54	-0.11
	>200	23442	14.59	21	8.71	-0.4
Distance from Roads (m)	0-50	45379	28.25	56	23.24	-0.18
	50-100	30591	19.04	50	20.75	0.08
	100-150	22536	14.03	33	13.69	-0.02
	150-200	17410	10.84	34	14.11	0.23
	200-250	12412	7.73	28	11.62	0.33
	250-300	9539	5.94	8	3.32	-0.44
	>300	22639	14.09	32	13.28	-0.06

Table 2 Spatial relationship between each landslide conditioning factor and landslide by index of entropy Model

Factor	Class	Percentage of domain	Percentage of landslide	P_{ij}	(P_{ij})	H_j	H_{jmax}	I_j	W_j
Slope gradient	0-15°	13.76	2.49	0.18	0.04	2.05	2.32	0.12	0.101
	15-25°	19.01	18.67	0.98	0.22				
	25-35°	26.47	35.68	1.35	0.31				
	35-45°	25.33	36.51	1.44	0.33				
	>45°	15.42	6.64	0.43	0.1				
Slope aspect	Flat	0.75	0	0	0	2.23	3.17	0.3	0.287
	North	18.12	12.86	0.71	0.08				
	North East	11.77	8.3	0.71	0.08				
	East	7.7	10.37	1.35	0.15				
	South East	7.43	12.86	1.73	0.2				
	South	11.3	17.84	1.58	0.18				
	South West	13.1	14.94	1.14	0.13				
	West	14.74	12.03	0.82	0.09				
	North West	15.02	10.79	0.72	0.08				
Plan Curvature (100/m)	Concave	45.74	47.3	1.03	0.51	1	1.58	0.37	0.249
	Flat	1.32	0	0	0				
	Convex	52.85	52.7	1	0.49				
Elevation	<300	15.83	17.84	1.13	0.19	1.59	3	0.47	0.344
	300-500	21.6	30.29	1.4	0.24				
	500-650	16.97	19.5	1.15	0.2				
	650-800	15.89	16.18	1.02	0.17				
	800-950	15.51	7.88	0.51	0.09				
	950-1100	12.32	8.3	0.67	0.11				
	1100-1250	1.47	0	0	0				
	>1250	0.42	0	0	0				
SPI	0-150	8.84	3.32	0.38	0.1	1.89	2	0.06	0.052
	150-300	12.29	16.18	1.32	0.36				
	300-450	9.22	8.72	0.95	0.26				
	>450	69.65	71.78	1.03	0.28				
TWI	<8	54.15	61.41	1.13	0.42	1.54	1.58	0.03	0.025
	10	32.22	30.29	0.94	0.35				
	>10	13.62	8.3	0.61	0.23				
STI	0-40	13.86	7.05	0.51	0.13	1.92	2	0.04	0.039
	40-80	19.01	22.82	1.2	0.3				
	80-120	15.87	21.16	1.33	0.33				
	>120	51.27	48.96	0.95	0.24				
Land Use	Barren	0.14	0	0	0	1.92	3.17	0.39	0.174
	Bush	24.27	16.6	0.68	0.17				
	Cultivation	30.98	48.55	1.57	0.39				
	Cutting	0.08	0	0	0				
	Forest	0.62	0	0	0				
	Grass	42.77	34.02	0.8	0.2				
	Orchard	0.9	0.83	0.92	0.23				
	River	0.16	0	0	0				
	Sand	0.003	0	0	0				
Lithology	Amphibolite	0.38	0.415	1.09	0.05	2.45	3.46	0.29	0.536
	Benighat Slate	10.1	9.96	0.99	0.05				
	Dandagaun Formation	0.53	0	0	0				
	Dhading Dolomite	16.63	10.79	0.65	0.03				
	Fagfog Quartzite	0.6	0.83	1.38	0.07				
	Kuncha Formation	1.24	0.41	0.33	0.02				
	Lower Siwaliks	1.55	4.15	2.68	0.13				
	Middle Siwaliks	0.04	0.41	10.3	0.51				
	Nourpul Formation	51.11	50.62	0.99	0.05				
	Purebesi Quartzite	0.81	0.41	0.51	0.03				
	Terrace Deposits	16.94	22.82	1.35	0.07				
Distance to Faults (m)	0-100	15.83	13.69	0.86	0.13	2.57	2.58	0.01	0.008
	100-200	13.88	17.43	1.26	0.2				
	200-300	12.95	14.11	1.09	0.17				
	300-400	11.04	12.45	1.13	0.18				
	400-500	9.42	12.03	1.28	0.2				
	>500	36.8	30.29	0.82	0.13				
Distance to Rivers (m)	0-50	34.23	41.49	1.21	0.26	2.29	2.32	0.01	0.014
	50-100	24.01	24.07	1	0.21				
	100-150	16.35	16.18	0.99	0.21				
	150-200	10.74	9.54	0.89	0.19				
	>200	14.59	8.71	0.6	0.13				
Distance to Roads (m)	0-50	28.25	23.24	0.82	0.11	2.75	2.81	0.02	0.021
	50-100	19.04	20.75	1.09	0.15				
	100-150	14.03	13.69	0.98	0.14				
	150-200	10.84	14.11	1.3	0.18				
	200-250	7.73	11.62	1.5	0.21				
	250-300	5.94	3.32	0.56	0.08				
	>300	14.09	13.28	0.94	0.13				

Table 3 Coefficients of each thematic map used in logistic regression modelin

Factor	Class	β
Slope		0.0214
Aspect	Flat	-13.2269
	North	-0.106
	Northeast	0.1073
	East	0.8568
	Southeast	0.3029
	South	0.5532
	Southwest	0.1169
	West	-0.1373
	Northwest	0
Curvature		0.0221
SPI		0.038
TWI		-0.2813
Lithology	Terrace Deposits	0.606
	Middle Siwaliks	2.369
	Lower Siwaliks	591
	Benighat Slate	0.369
	Dhading Dolomite	-0.598
	Nourpul Formation	0.294
	Purebesi Quartzite	-0.341
	Amphibolites	0.127
	Dandagaun Formation	-14.34
	Fagfog Quartzite	-14.511
	Kuncha Formation	0
Land use	Barren	14.447
	Bush	12.814
	Cultivation	13.445
	Cutting	-1.555
	Forest	-1.508
	Grass	12.954
	Orchard	13.108
	River	-1.264
	Sand	0
Distance form fault		-0.000041
Distance form road		-0.00038
Distance form river		-0.0004

Table 4 Parameters for the calculation of ROC curve (modfied from Swets 1988)

	Landslide bodies	Landslide free areas
Landslide occurrence based on calculated function	True positive (TP)	False positive (FP)
Safe areas based on calculated function	False negative (FN)	True negative (TN)

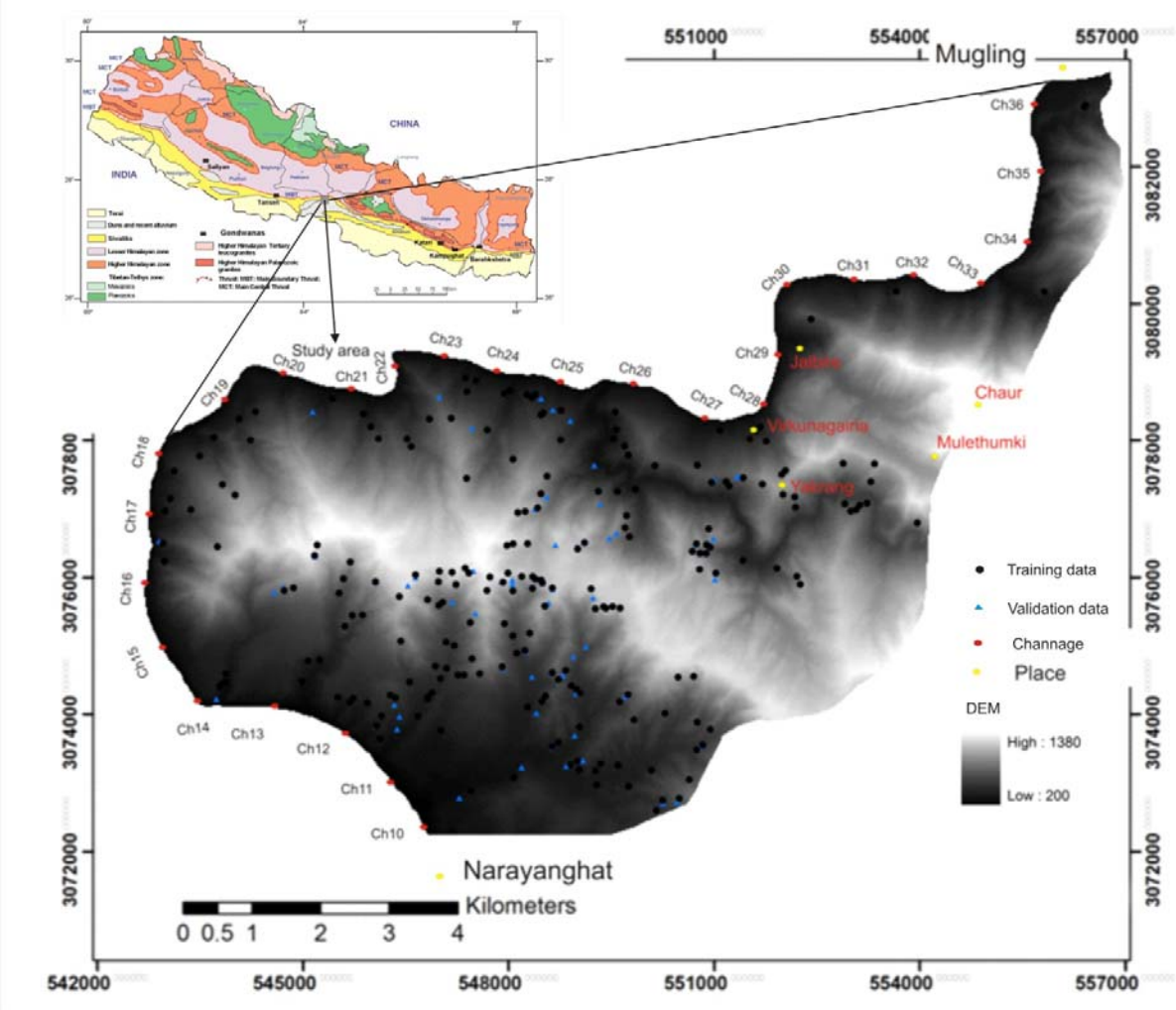

Fig.1: Study area with the distribution of landslides

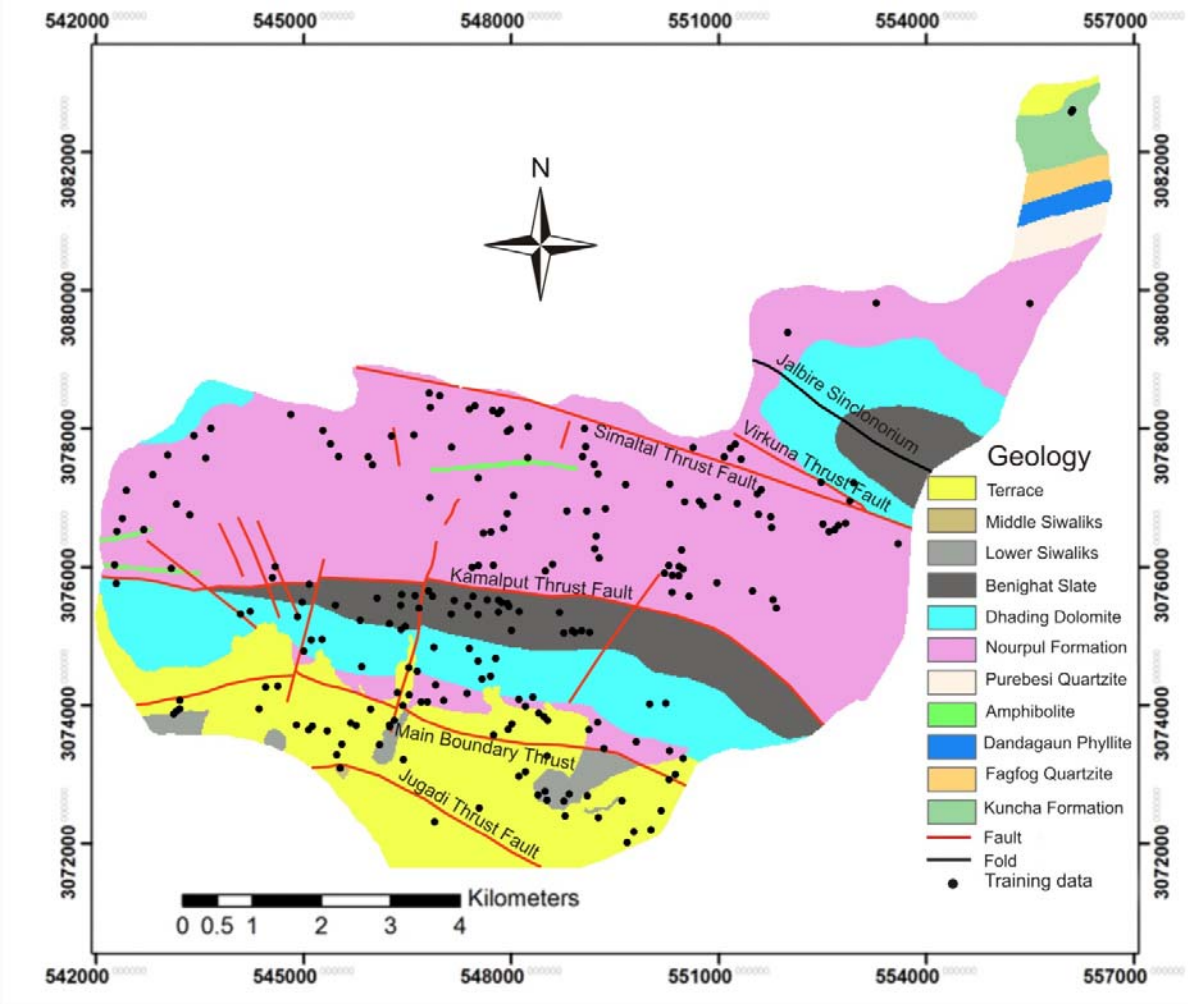

Fig.2: Geological map of the study area


19 13:31

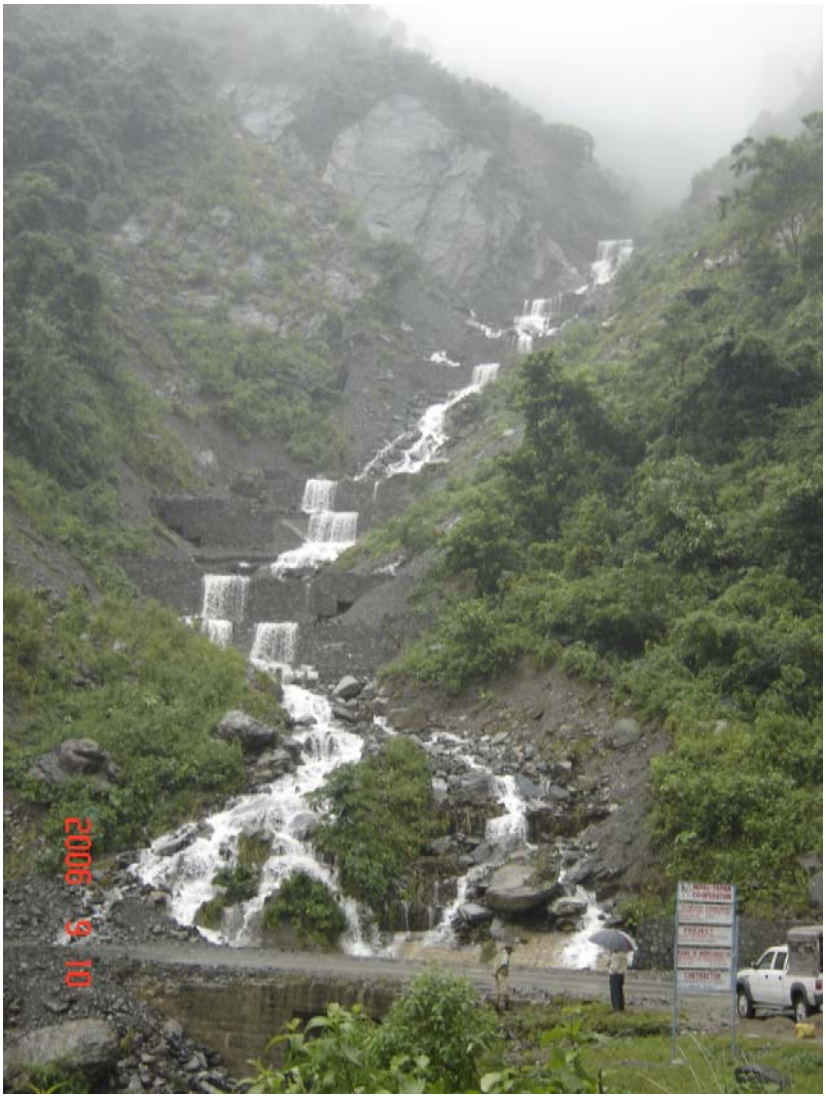
2006 9 10

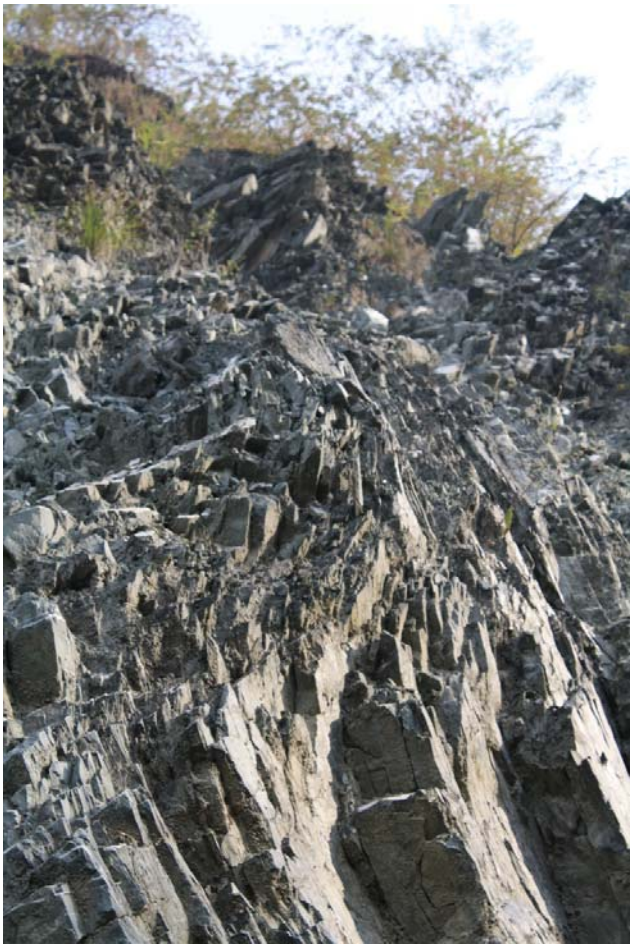

Fig.3: Figure showing different types of landslides observed in the study area (a) Thick debris deposit which buried the bridge over the road section, at 21+500 km; (b), Landslide at 23+760 km of the road section (c) Debris slide observed at 20+800 km of the road section (L2) (d) Rock topple observed at the upstream of Keraghari Khola, at 21+560 km; (e)Slope failure observed at 30+500 km.

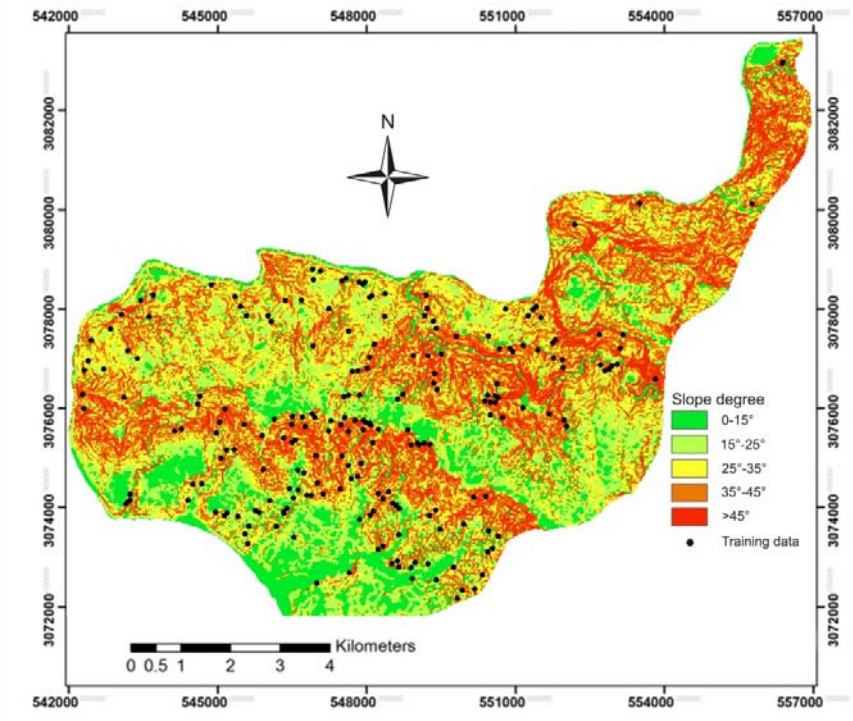

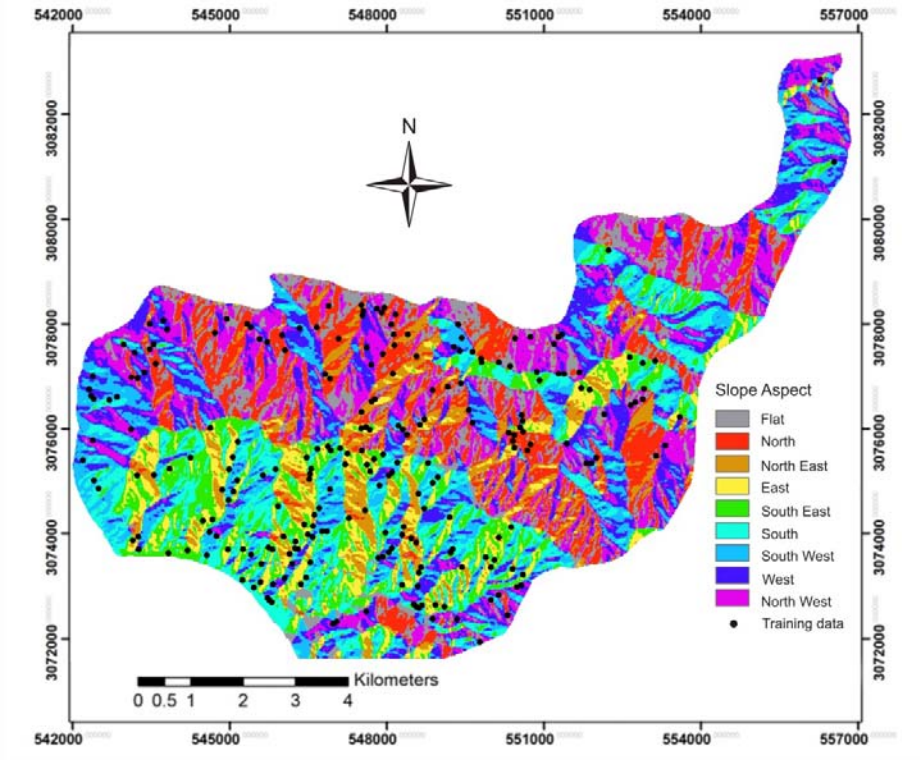
542000
545000
548000
551000
554000
557000
3082000
3080000
3078000
3076000
3074000
3072000
N
Slope Aspect
Flat
North
North East
East
South East
South
South West
West
North West
Training data
Kilometers
0 0.5 1 2 3 4

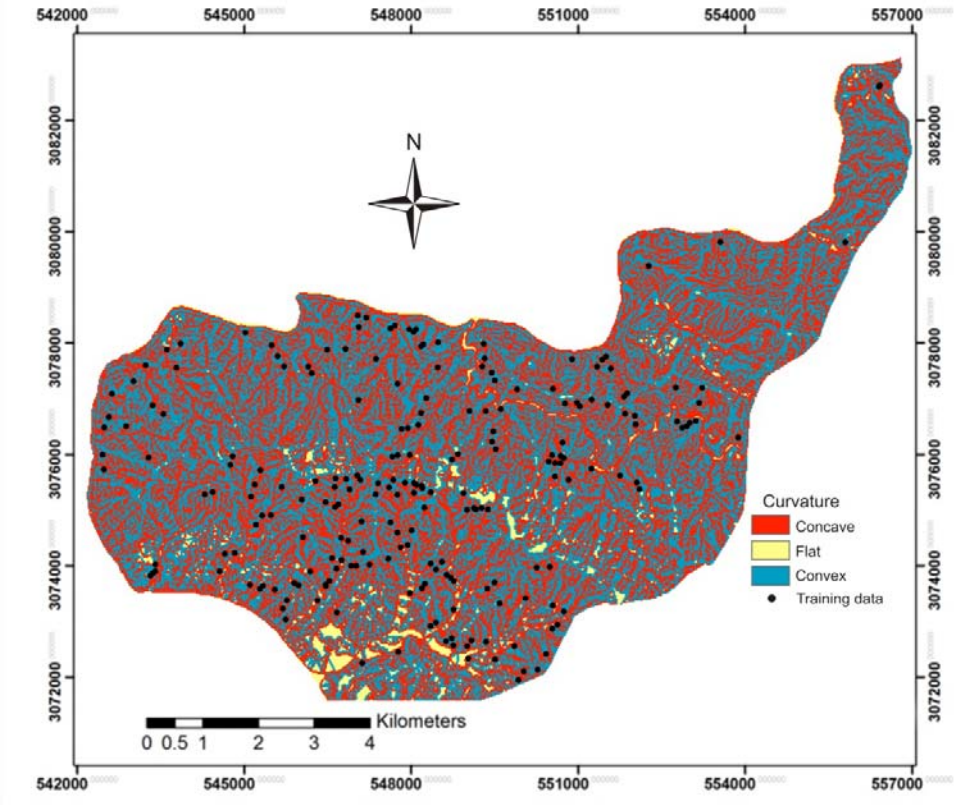
542000
545000
548000
551000
554000
557000
3082000
3080000
3078000
3076000
3074000
3072000
N
Curvature
Concave
Flat
Convex
Training data
Kilometers
0 0.5 1 2 3 4

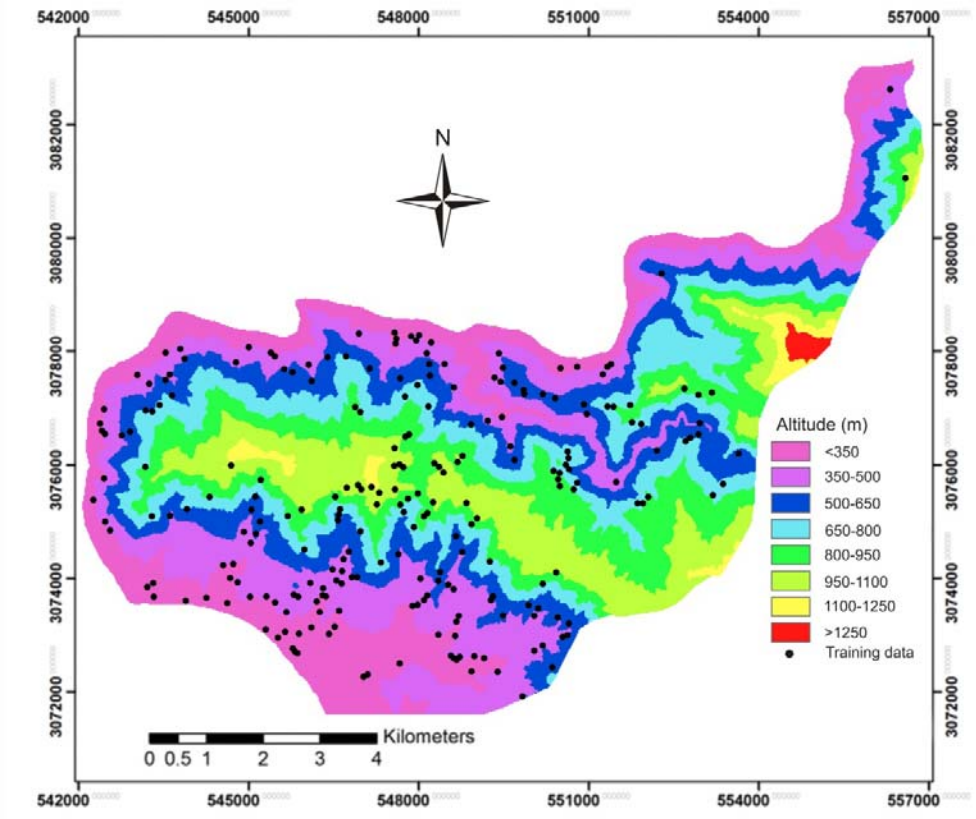
542000
545000
548000
551000
554000
557000
3082000
3080000
3078000
3076000
3074000
3072000
N
Altitude (m)
<350
350-500
500-650
650-800
800-950
950-1100
1100-1250
>1250
Training data
Kilometers
0 0.5 1 2 3 4

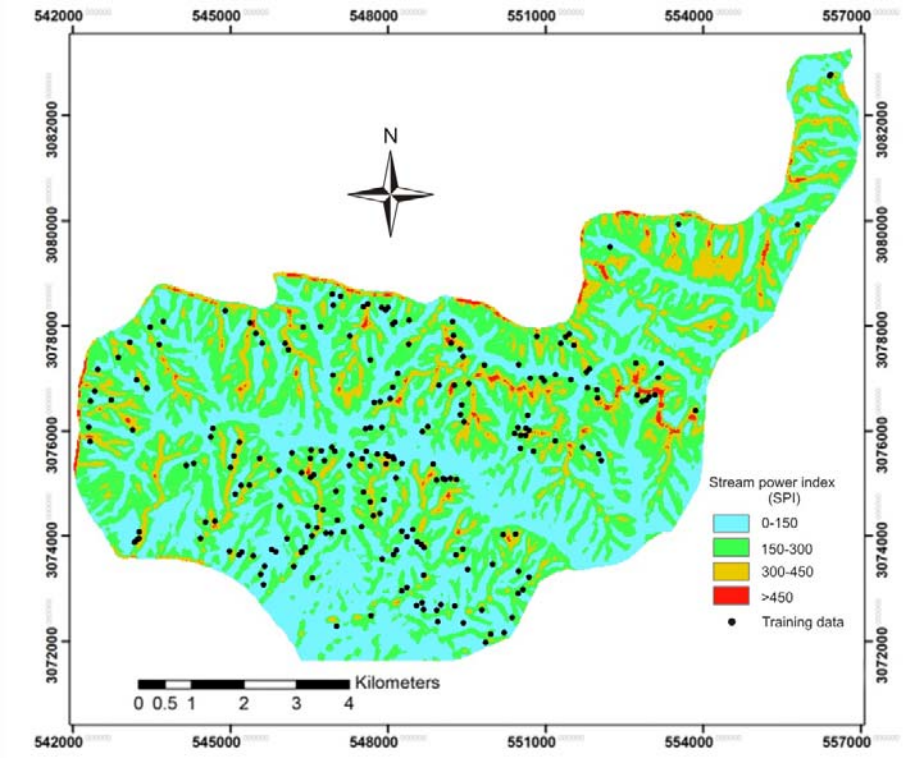
542000
545000
548000
551000
554000
557000
3082000
3080000
3078000
3076000
3074000
3072000
N
Stream power index
(SPI)
0-150
150-300
300-450
>450
Training data
Kilometers
0 0.5 1 2 3 4

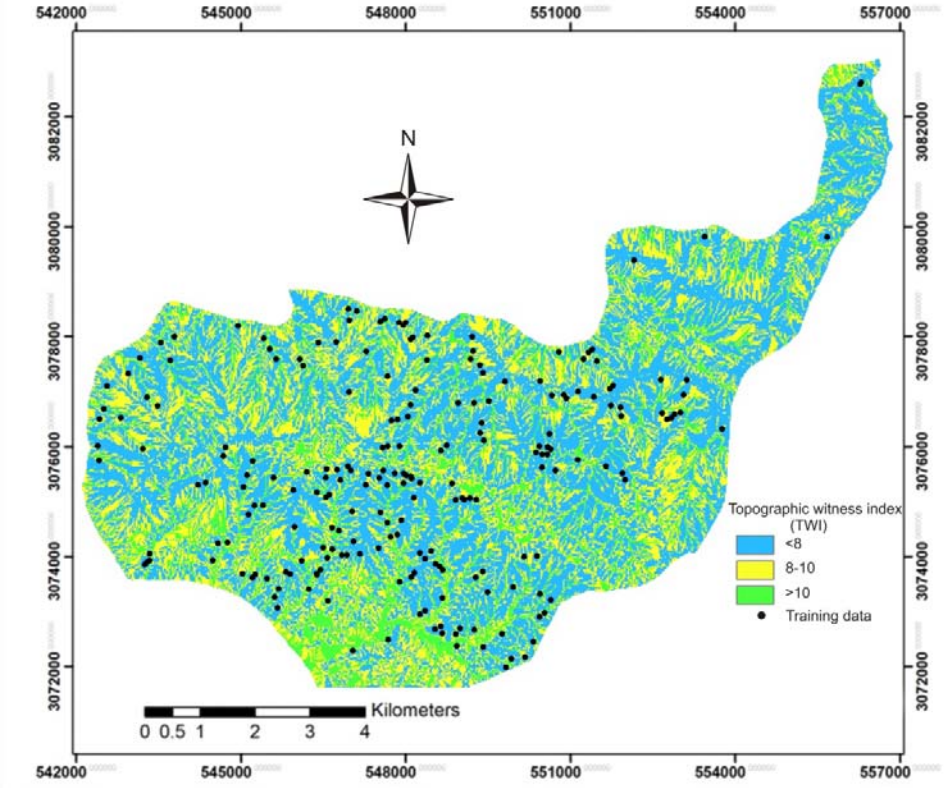
542000
545000
548000
551000
554000
557000
3082000
3080000
3078000
3076000
3074000
3072000
N
Topographic witness index
(TWI)
<8
8-10
>10
Training data
Kilometers
0 0.5 1 2 3 4

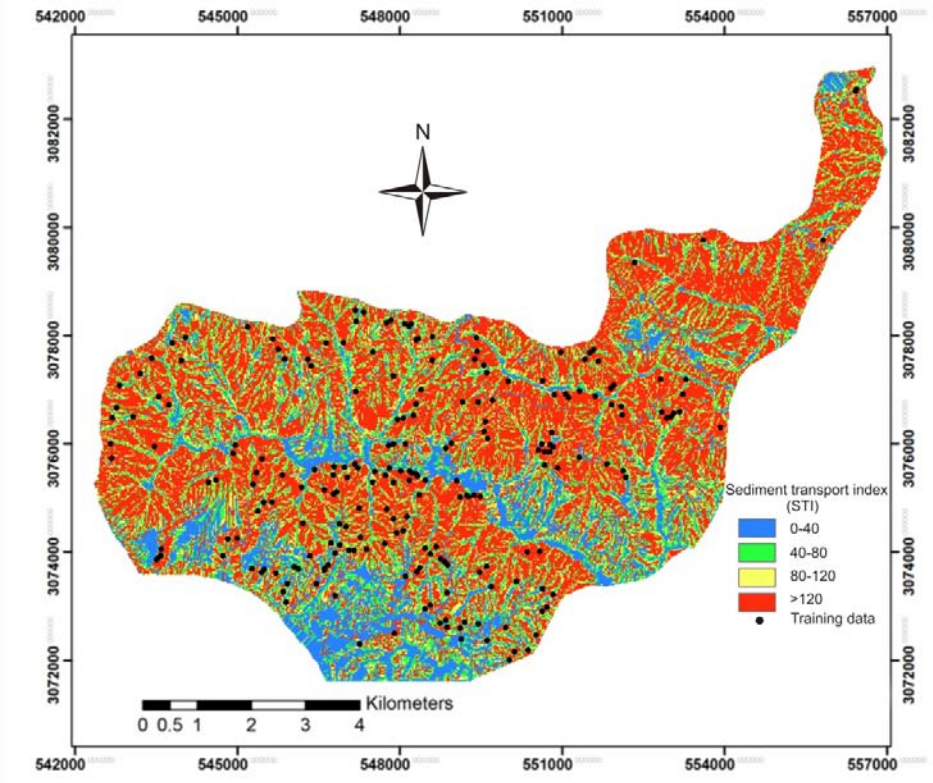
542000
545000
548000
551000
554000
557000
3082000
3080000
3078000
3076000
3074000
3072000
N
Sediment transport index (STI)
0-40
40-80
80-120
>120
Training data
Kilometers
0 0.5 1 2 3 4

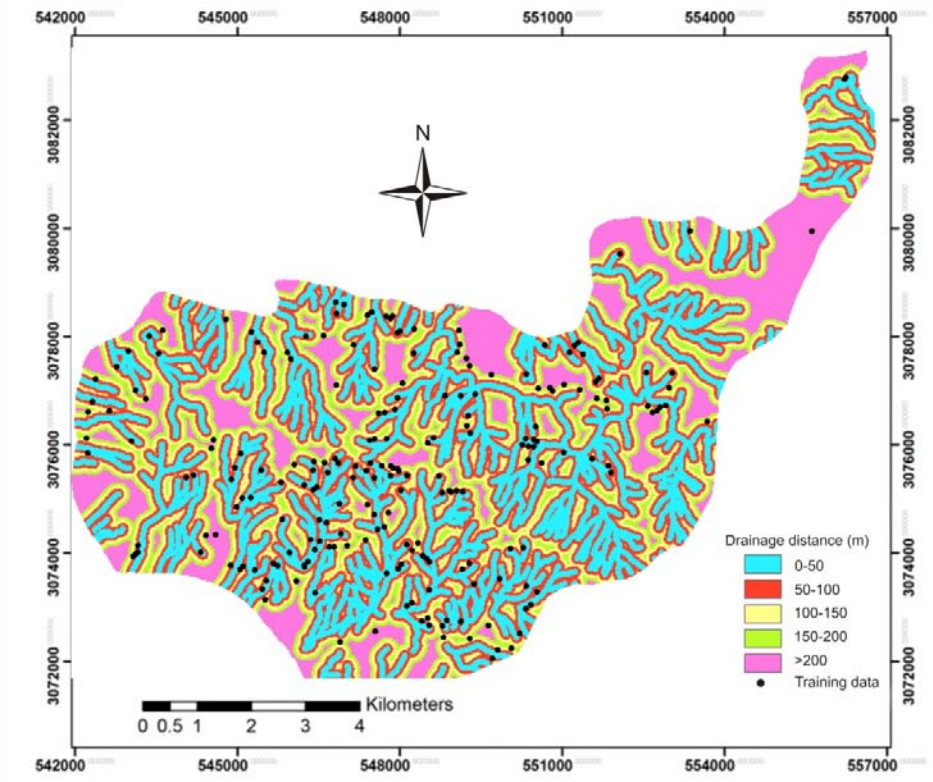
542000
545000
548000
551000
554000
557000
3082000
3080000
3078000
3076000
3074000
3072000
N
Drainage distance (m)
0-50
50-100
100-150
150-200
>200
Training data
Kilometers
0 0.5 1 2 3 4

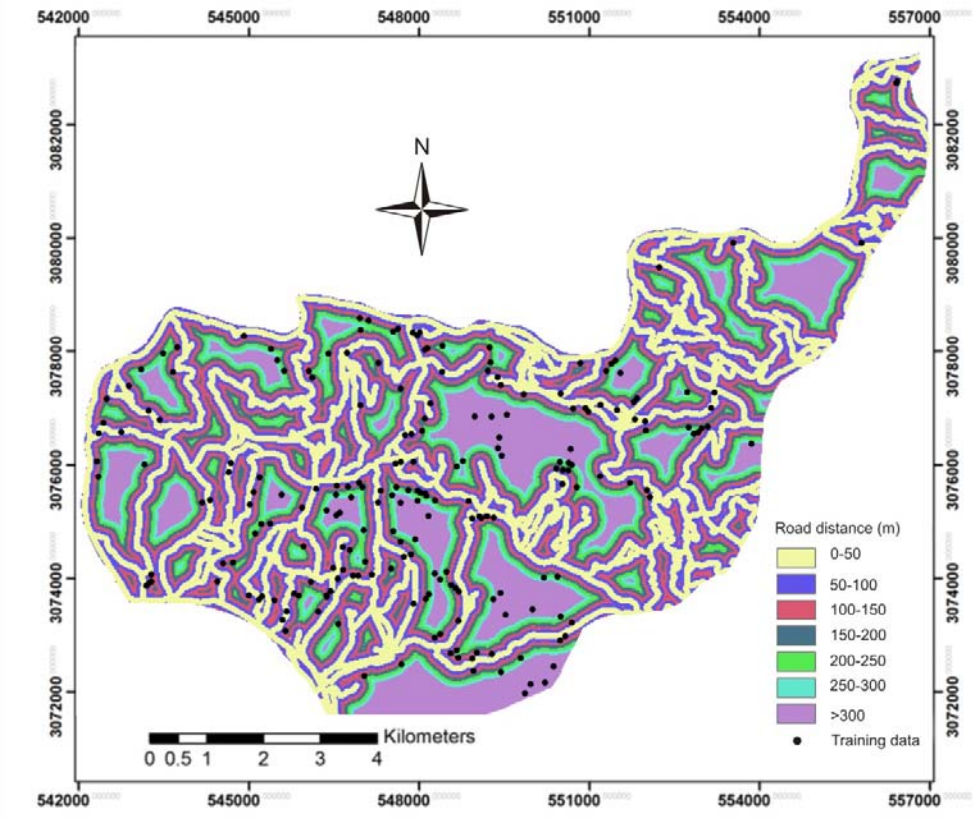
542000
545000
548000
551000
554000
557000
3082000
3080000
3078000
3076000
3074000
3072000
N
Road distance (m)
0-50
50-100
100-150
150-200
200-250
250-300
>300
Training data
Kilometers
0 0.5 1 2 3 4

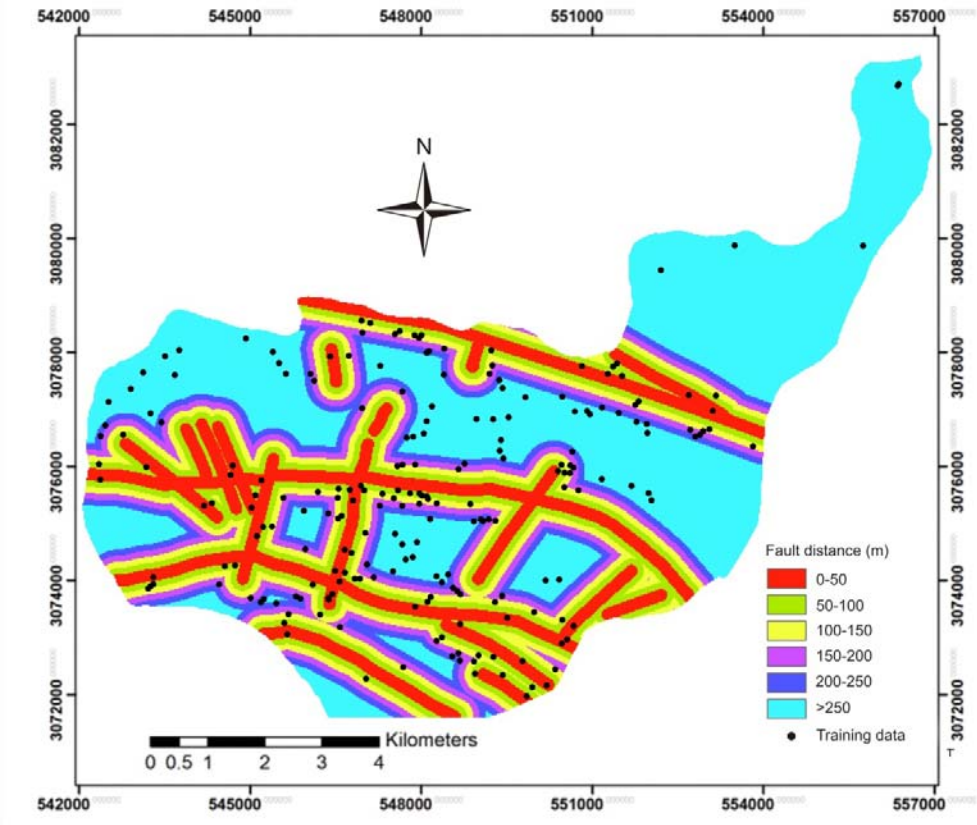
542000
545000
548000
551000
554000
557000
3082000
3080000
3078000
3076000
3074000
3072000
N
Fault distance (m)
0-50
50-100
100-150
150-200
200-250
>250
Training data
Kilometers
0 0.5 1 2 3 4

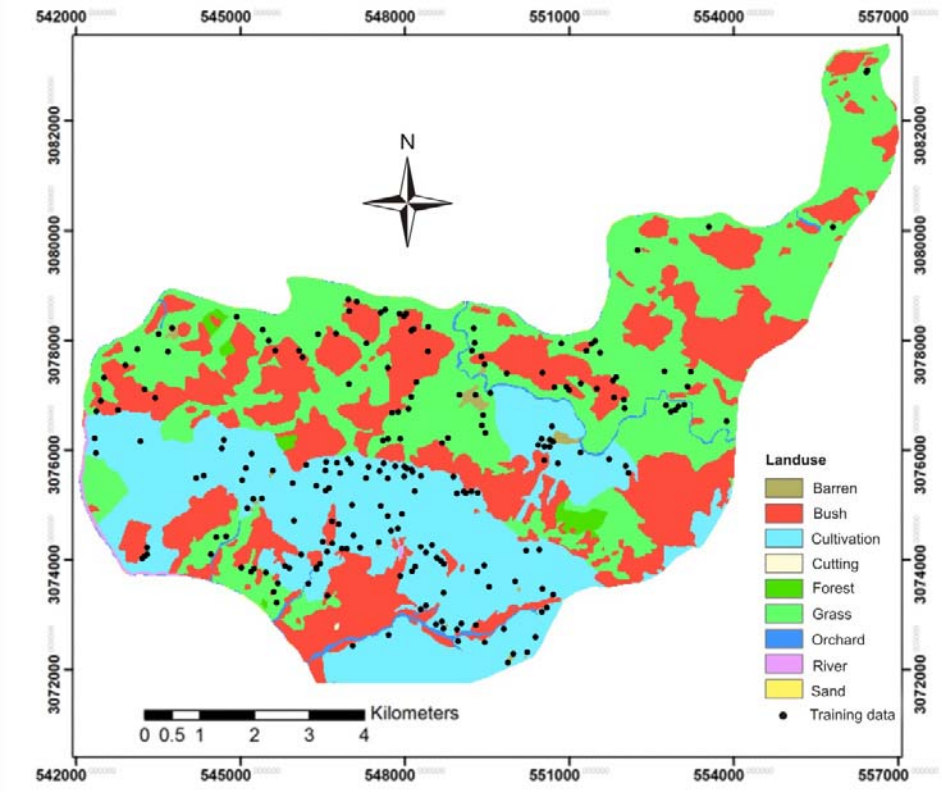

Fig.4: Various thematic maps used for the present study (a) Slope map (in degree), (b) Aspect map, (c) Curvature map, (d) Elevation map (in meter), (e) Stream power Index map, (f) Topographic Witness Index map (g) Sediment Transport Index map (h) Drainage map (distance in meter), (i) Road map (distance in meter), (j) Fault distance map (distance in meter) (k) Land use map

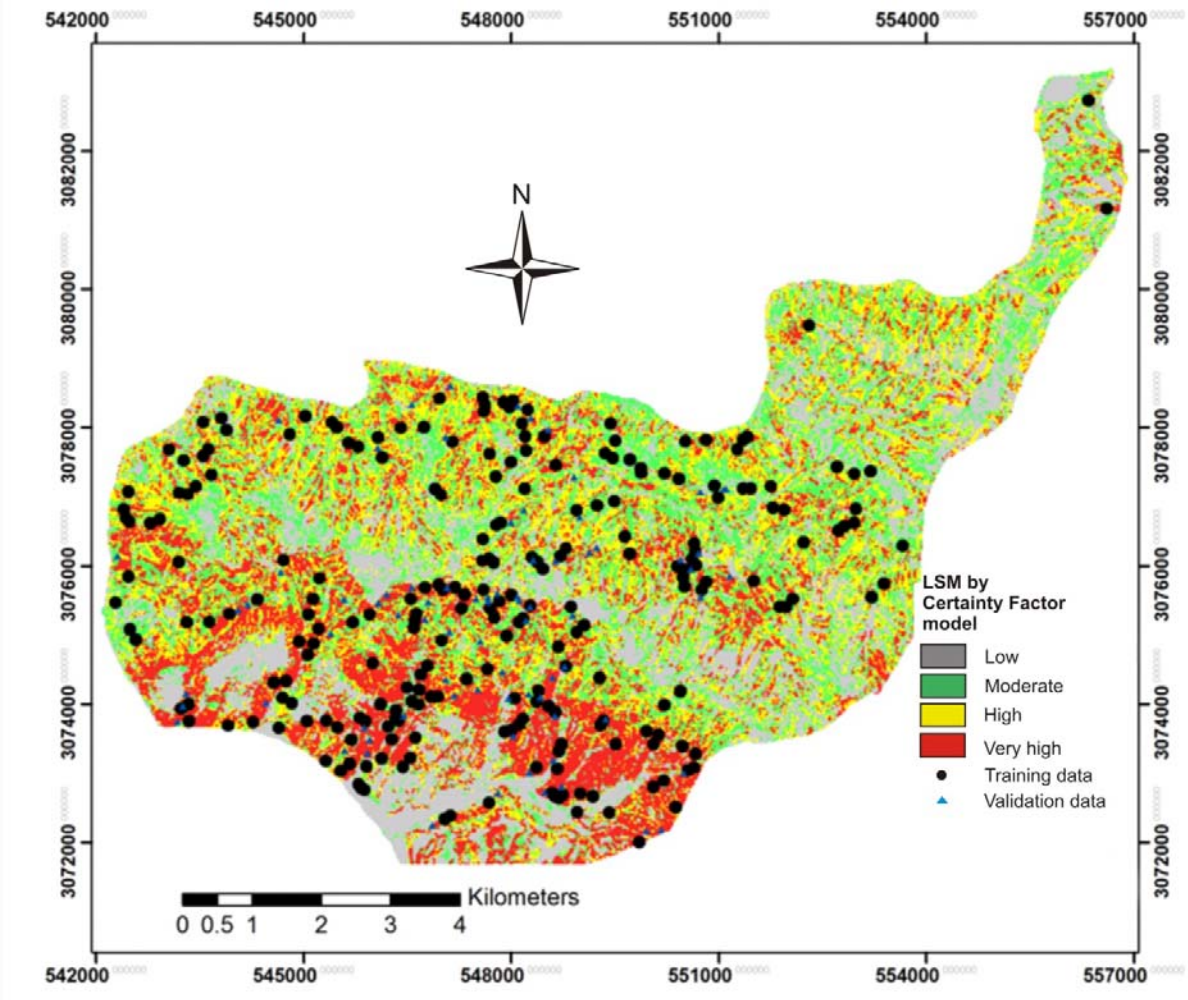

Fig. 5: Landslide susceptibility map based on certainty factor (CF) model

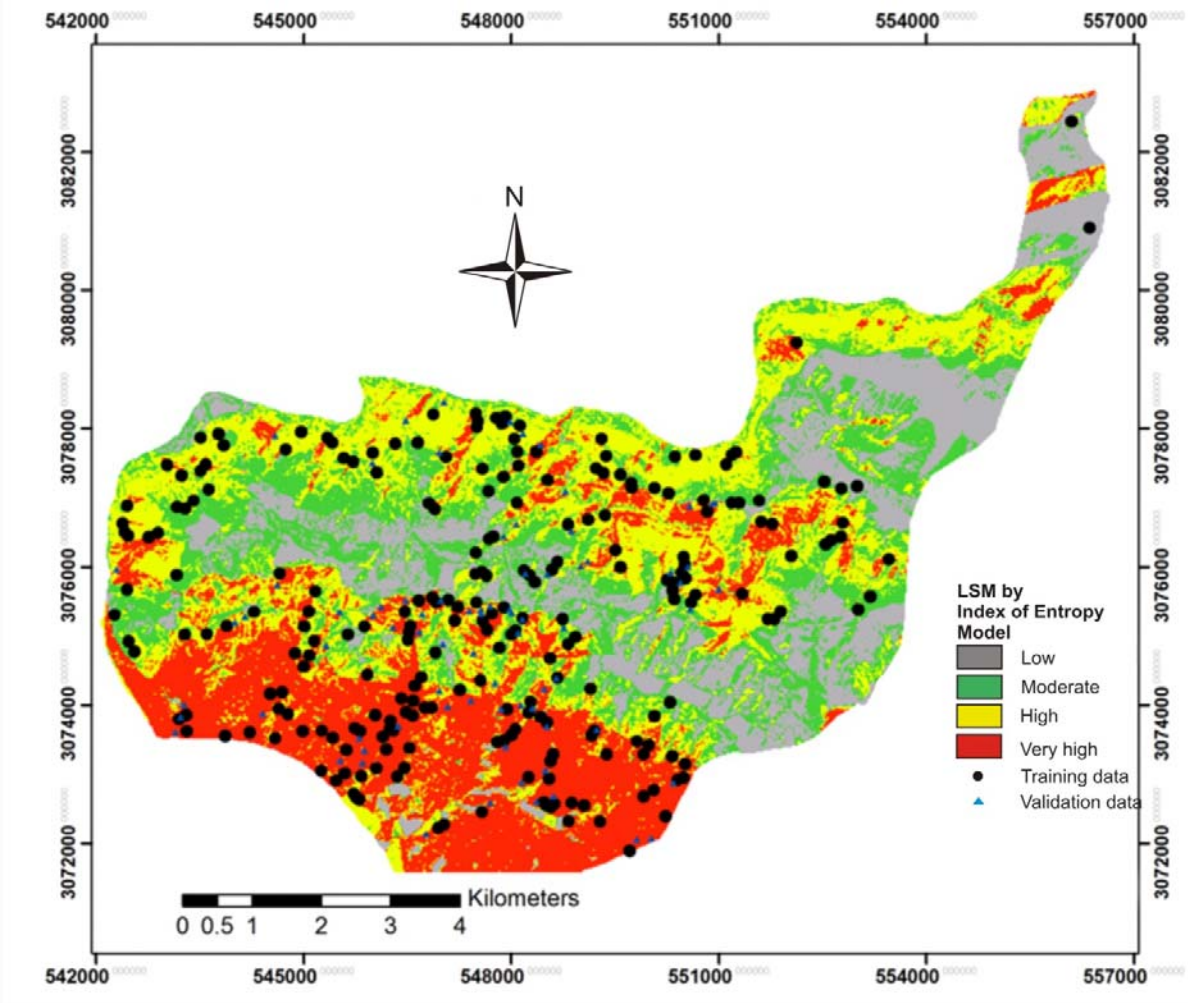

Fig.6. Landslide susceptibility map derived from the index of entropy (IOE) model.

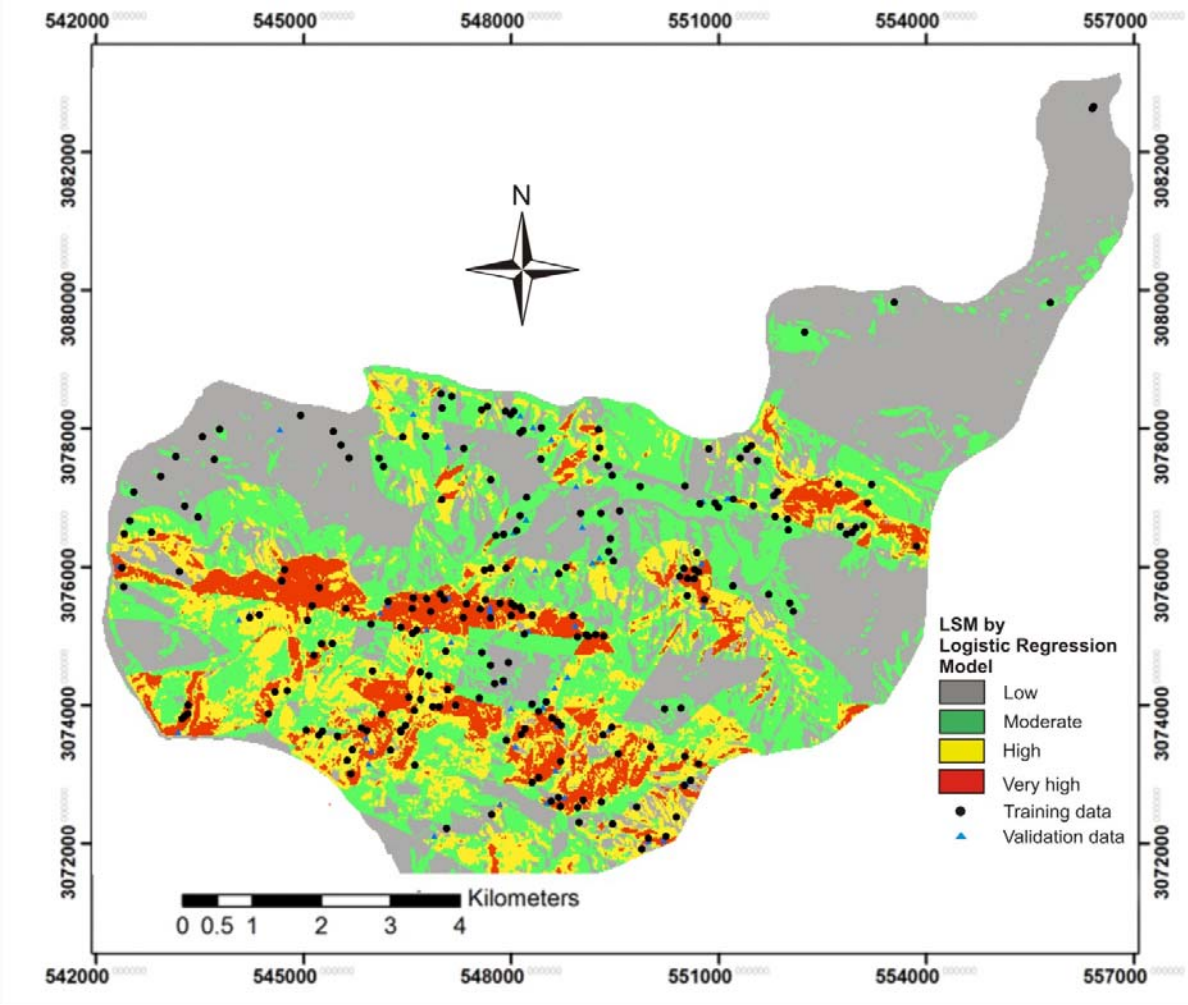

Fig. 7: Landslide susceptibility map derived from the logistic regression (LR) model.

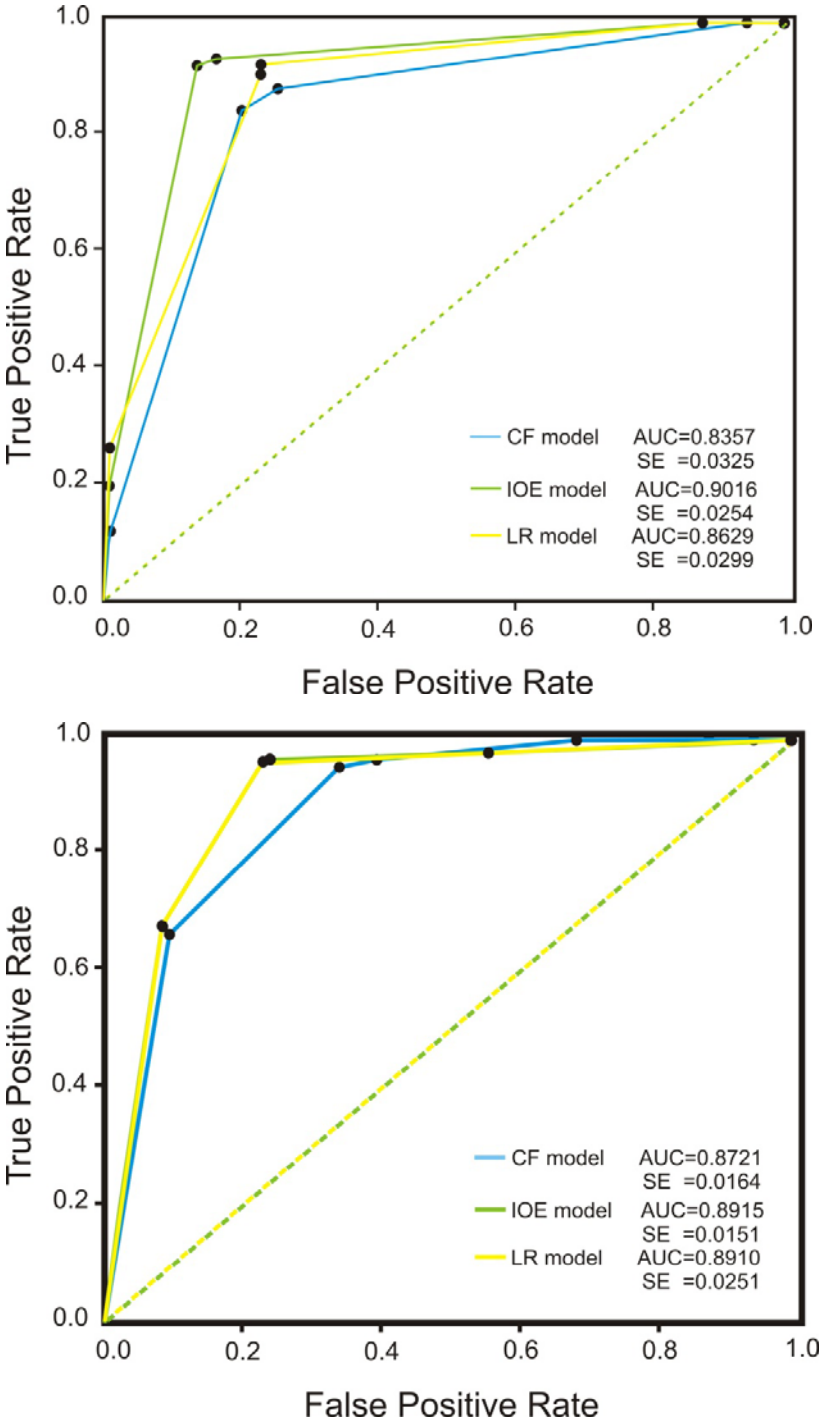

Fig. 8 ROC curve and area under the curve (a) Prediction rate models (b) Success rate models for certainty factor (CF) model, index of entropy (IOE) model and logistic regression (LR) model